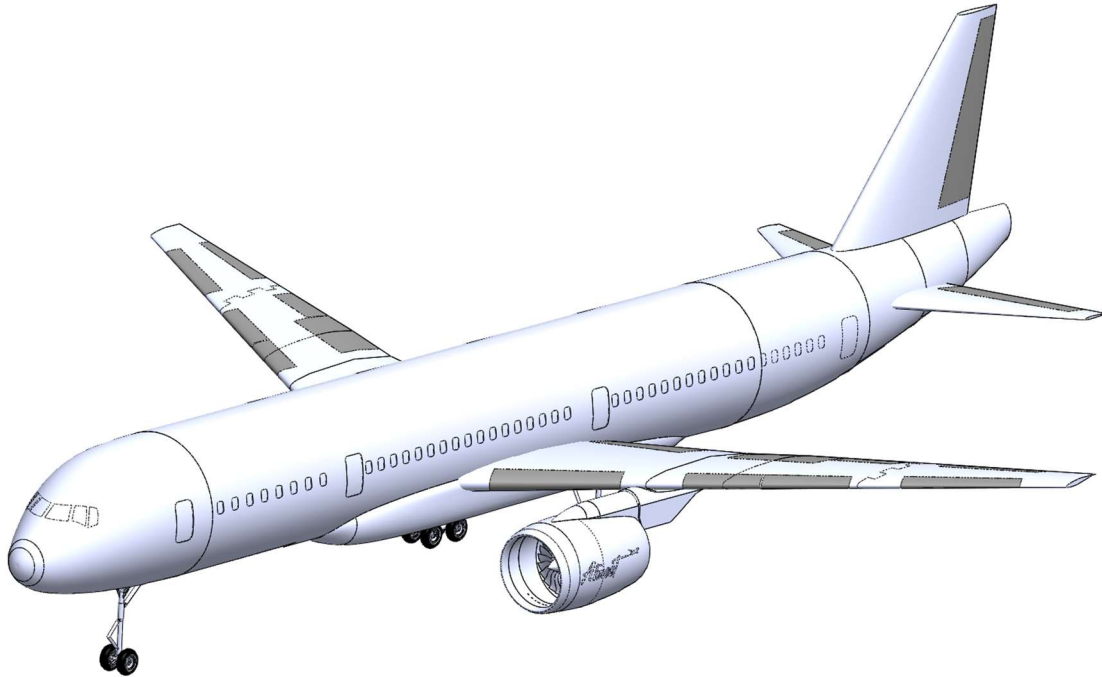


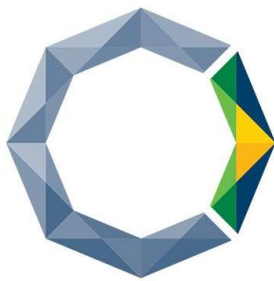


Atmospheric Travel, Connecting the World

“Songbird”







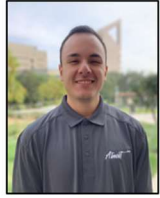




AIAA 2019 – 2020 Undergraduate Team Air Vehicle Design Competition
in response to the to the AIAA High Capacity Short Range Aircraft Proposal


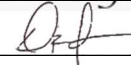
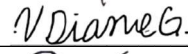
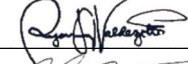
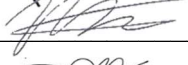


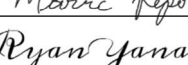
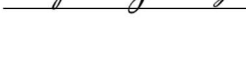


CalPolyPomona

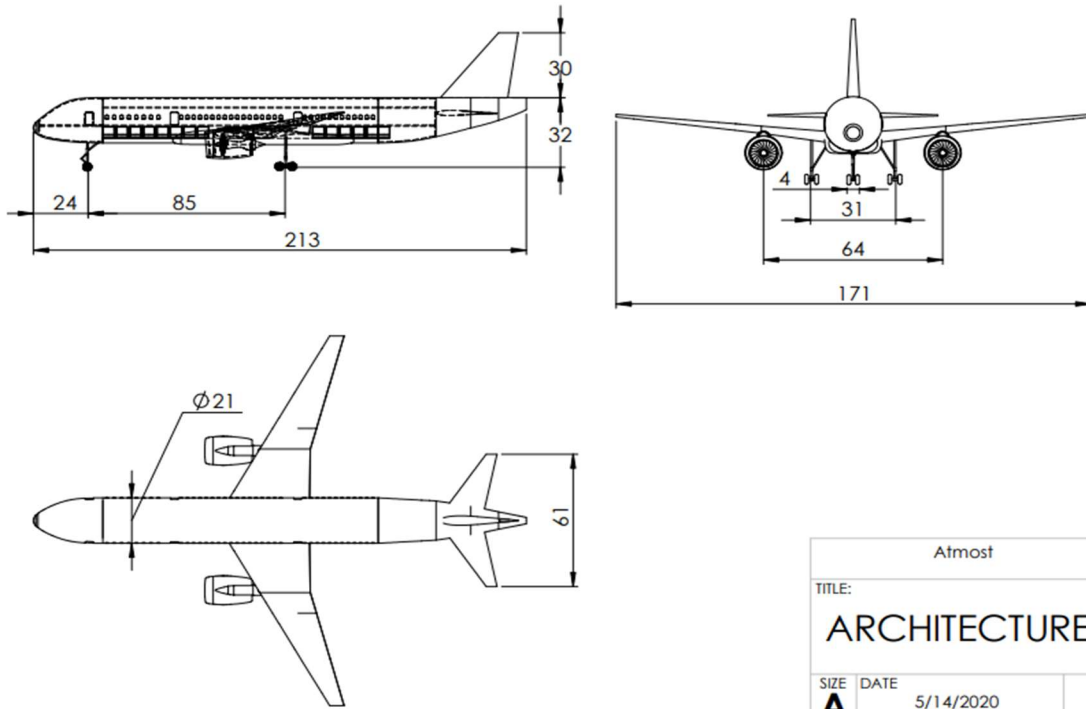
Presented by California State Polytechnic University – Pomona
Aerospace Engineering Department

Team Organization

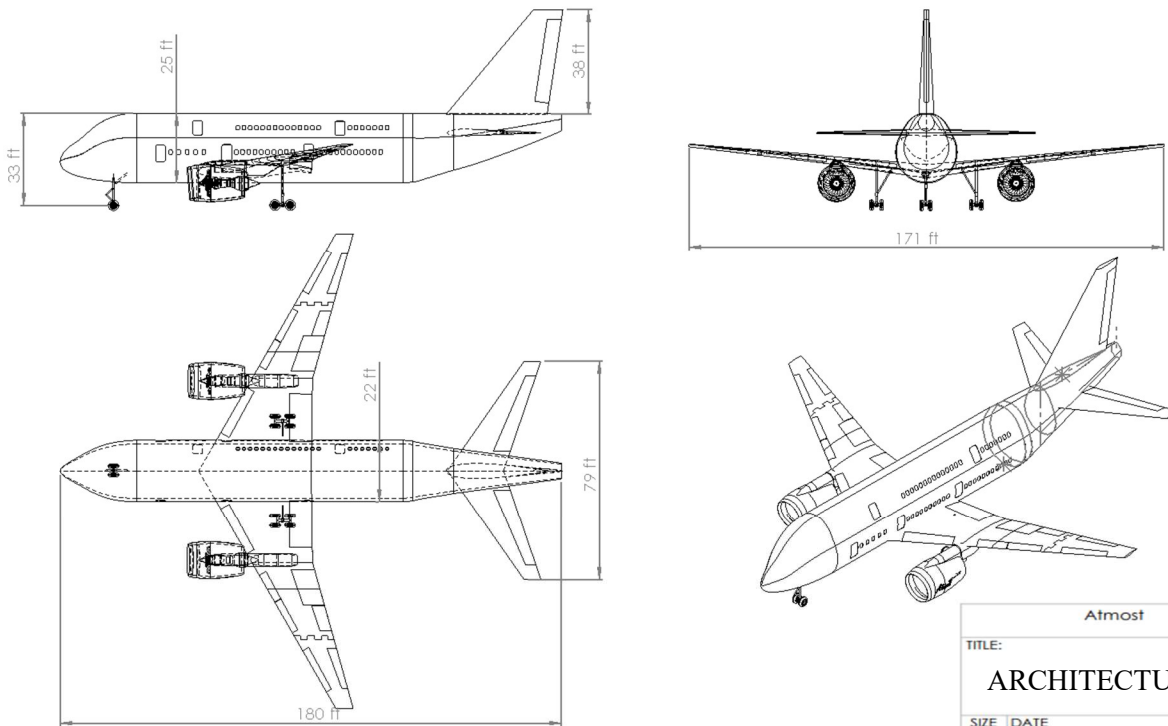
 Sean McGowan Team Lead Trade Studies	 Demetrious Jarvis Lead Deputy Performance	 Vanessa Gonzalez Cost Analysis Performance Trade Studies
 Ryan Valdezotto Weight & Balance Performance	 Max Ayala CAD Modeling Structures	 Daniel Kim Aerodynamics Structures
 Abram Ghobrial CAD Modeling Trade Studies	 Marc Repollo Aerodynamics Propulsion	 Ryan Yanagi Aerodynamics Stability & Control

<u>Name</u>	<u>Email</u>	<u>AIAA Number</u>	<u>Signature</u>
Sean McGowan	somcgowan@cpp.edu	1087158	
Demetrious Jarvis	drjarvis@cpp.edu	1109471	
Vanessa Gonzalez	vdgonzalez@cpp.edu	1109472	
Ryan Valdezotto	ravaldezotto@cpp.edu	1082164	
Max Ayala	mfayala@cpp.edu	1109475	
Daniel Kim	danielkim2@cpp.edu	1109470	
Abram Ghobrial	ighobrial@cpp.edu	1086828	
Marc Repollo	mdrepollo@cpp.edu	1109266	
Ryan Yanagi	rtyanagi@cpp.edu	1109593	
Dr. Donald Edberg (Advisor)	dedberg@cpp.edu	22972	

3-View Photo of Both Architectures



Atmost		
TITLE: ARCHITECTURE 1		
SIZE A	DATE 5/14/2020	
Units: ft*	SCALE: 1:500	SHEET 1 OF 1



Atmost		
TITLE: ARCHITECTURE 2		
SIZE A	DATE 5/14/2020	
Units: ft*	SCALE: 1:500	SHEET 1 OF 1

Executive Summary

In response to the 2019-2020 American Institute of Aeronautics and Astronautics (AIAA) Undergraduate Team Aircraft Design Competition Request for Proposal (RFP), Atmospheric Travel, AtmosT, presents the Songbird. A recurring problem that arises with the increase in air travel is the congestion of major commercial airports. This RFP is for the design of an aircraft that addresses this market problem. Specifically, a high capacity, short range transport aircraft designed to alleviate airport congestion, without the size and cost that comes with long range capability. The Songbird offers an economical innovation such as folding wing tips that are optimized to ensure proper gate sizing. Gate sizing is important because the Songbird will park in the same size gates as its current compared competition. This architecture will accommodate twice as many passengers per gate.

The Songbird and Double ECO were designed to accomplish such task. Songbird was designed to be simple and cost efficient to produce. This aircraft also is very safe and reliable and offers an option for side-slip seating to reduce boarding time which results in more flights per day. Double ECO was designed to reduce size to fit into gates easier and maximize usage of the fuselage volume. This architecture allows for multiple entry points which also reduces boarding time. Both aircraft demonstrate folding wings in order to fit gate constraints. Since this aircraft aims to replace category III aircraft, it is necessary to be able to fit into category III terminals since the vacancy will need to be filled. Designing an aircraft that fits into a category V terminal would only add to congestion at these gates. This will be covered in section 3.2

This report covers major decisions and processes in designing such an aircraft within the scope of current infrastructure and technological developments.

Table of Contents

Team Organization	i
3-View Photo of Both Architectures	1
Executive Summary	2
Table of Contents	3
List of Acronyms	7
List of Figures	9
List of Tables	11
1.0 Requirements Overview	12
2.0 Compliance Matrix	13
3.0 Design Approach	15
3.1 Mission Marketing Study	15
3.2 Concept of Operations	18
3.3 Mission Profile (3500 and 700 DRM)	22
4.0 Trades of Major Design Components and Final Architecture Selection	24
4.1 Side Slip Seats	24
4.2 BLI Engine	26
4.3 Strut Braced and Box Wing Designs	27
4.4 Various Fuselages	28
4.5 Configuration/Down Select	29
5.0 Cost Estimate	32
5.1 Development and Production Cost	32
5.2 Direct Operating Cost	35
5.3 Cost Estimate Summary and Comparison	37
6.0 Graphical Representation	39
6.1 Justification for Diagram (Alt-Mach Trade)	39
6.2 Design Point (Constraint Diagram)	39
6.3 Initial Maximum Takeoff Weight	40
7.0 Geometric Drawings	43
7.1 Scaled 3-View	43
7.2 Internal Volume Requirements	43
7.2.1 Fuel Tank	43
7.2.2 Cargo Container	44
7.3 Cross-section showing passenger seats Layout of passenger	45

7.4 Layout of Cockpit	46
7.5 Fuselage centerline diagram	47
8.0 Aircraft Weight Statement.....	48
8.1 Weight Breakdown	48
8.2 CG travel using the CG boundaries as defined in the notch chart	49
9.0 Propulsion System.....	51
9.1 Propulsion Trade Study	51
9.2 Final Engine Selection and Justification.....	55
10.0 Aircraft Innovation: Folding Wingtip	57
11.0 Aerodynamic Characteristics and Performance.....	Error! Bookmark not defined.
11.1 Airfoil Selection	59
11.2 Lift Curve Slopes.....	60
11.3 Drag Polar.....	61
12.0 Performance	63
12.1 Takeoff Field Length	63
12.2 Landing Field Length	65
12.3 Flight Envelope.....	66
12.4 Payload Range.....	67
13.0 Structures.....	68
13.1 V-N Diagram	68
13.2 Spar and Rib Sizing	69
13.3 Material Selection	70
14.0 Landing Gear	71
14.1 Landing Gear Placement.....	71
14.2 FAA Requirements for Tip back/ Roll Over etc.	71
14.3 Tire selection.....	73
15.0 Stability Control.....	74
15.1 Notch Chart	74
15.2 Control Surface Placement	74
15.3 AVL Analysis.....	75
15.4. Trim Condition	76
15.5 Stability Derivatives.....	78
16.0 Manufacturability and Reliability.....	79
16.1 Manufacturability	79

16.2 Reliability.....	80
17.0 Life Cycle Carbon Dioxide Emissions Estimate.....	83
17.1 Research on finding equations and existing numbers	83
17.2 Emissions comparison with significance	83
18.0 Conclusion	85
References.....	87

Acknowledgments

The 2019 – 2020 AtmosT Air Vehicle Design Team would like to thank the following professors at the California State Polytechnic University – Pomona for their advice and expertise in the field of Aerospace Engineering:

Dr. Donald Edberg – Aerospace Engineering Lead Faculty Advisor (CPP)

Professor Grant Carichner – Aerospace Engineering Air Vehicle Design Advisor (CPP)

Professor Steven Dobbs – Aerospace Engineering Program Management Advisor (CPP)

Professor Raymond Hudson – Aerospace Engineering Model Based Systems
Architecture Advisor (CPP)



List of Acronyms

Symbol	Definition
14 CFR	Title 14 Code of Federal Regulations
α	Angle of Attack
AC	Aerodynamic Center
AVL	Athena Vortex Lattice
AR	Aspect Ratio
ATC	Air Traffic Control
b	Wingspan (ft)
b_E	Span of Elevator (ft)
C.G	Center Gravity (ft)
C	Chord Length (ft)
C_D	Coefficient of Drag
C_E	Chord of Elevator (ft)
C_{HT}	Horizontal Tail Volume Coefficient
C_L	Coefficient of Lift
C_M	Coefficient of moment
C_m	Directional Stability Derivative
CO ₂	Carbon Dioxide
C_{VT}	Vertical Tail Volume Coefficient
CFR	Code of Federal Regulations
D	Drag (lb)
DOC	Direct Operating Cost
DRM	Design Reference Mission
EASA	European Union Aviation Safety Agency
FAA	Federal Aviation Administration
FAR	Federal Aviation Regulations
fpm	Feet Per Minute
HT	Horizontal Tail
IFR	Instrument Flight Rules
KCAS	Calibrated Airspeed (knots)

L	Lift (lb)
LE	Leading Edge
L/D	Lift-to-Drag ratio
MAC	Mean Aerodynamic Chord (ft)
MGTOW	Max Gross Takeoff Weight
MSL	Mean Sea Level
M_z	Lateral Moment (ft-lb)
M_z	Longitudinal Moment (ft-lb)
NACA	National Advisory Committee for Aeronautics
nmi	Nautical Miles
T/W	Thrust to Weight Ratio
q	Dynamic Pressure (lb/ft)
S	Wing Area (ft)
S_{HT}	Horizontal Tail Area (ft)
S_V	Vertical Tail Area (ft)
TE	Trailing Edge
t/c	Thickness Ratio
Tsfc	Thrust-Specific Fuel Consumption
VFR	Visual Flight Rules
VT	Vertical Tail
V_z	Shear Force
W/S	Wing Loading (psf)

List of Figures

Figure 1 - Most Frequently Flown to Airports Within 700 nmi from ATL	15
Figure 2 - MIT Research Shows CAT III is the most Utilized Gate Type.....	19
Figure 3 - Model Simulates Turn Time of Operations from Wheels Down to Wheels Up ..	20
Figure 4 - Decomposition of ground crew personnel.....	20
Figure 5 - critical path shown in green from wheels down to taxi out to the runway	21
Figure 6 - Design Range Mission	22
Figure 7 - Design Reference Mission	23
Figure 8 - Side Slip seating increases aisle width	24
Figure 9 - Songbird can save approximately 35 minutes at the airport	25
Figure 10 - Historical data trends of enplaning and deplaning on B-757 [16]	26
Figure 11 - Onera BLI Aircraft	27
Figure 12 - Aurora D8 BLI Aircraft	27
Figure 13 - Strut Braced Wing	28
Figure 14 - Boxed Wing Design	28
Figure 15 - Ecoliner Double Decker	28
Figure 16 - Boeing BWB.....	29
Figure 17 – Songbird	29
Figure 18 - Double ECO	30
Figure 19 - Breakdown of Development Cost using Two Methods	32
Figure 20 - Breakdown of Production Cost using Two Methods	33
Figure 21 - Breakeven for the Production of 500 Aircraft using Raymer’s Method.....	34
Figure 22 - Breakeven for the Production of 500 Aircraft using Nicolai & Carichner’s Method	35
Figure 23 - Breakdown of Direct Operating Cost for 700 nmi Mission.....	36
Figure 24 - Altitude-Mach Trade for Optimal Cruise Conditions for 700 nmi	39
Figure 25 - Constraint Diagram for Aircraft	40
Figure 26 - Empty Weight vs. Empty Weight Fraction.....	42
Figure 27 – 3-View of AtmosT Down Selected Aircraft	43
Figure 28 - Placement of Fuel Tanks.....	44
Figure 29 - Cargo Container	45
Figure 30 - Dimensions LD-3 Containers	45
Figure 31 – Layout of Passengers and Amenities	46
Figure 32 - Cockpit Layout of the A330.....	47
Figure 33 – Aircraft Centerline Diagram	47
Figure 34 - Fuselage group accounts for ~38% of the calculated refined empty weight	49
Figure 35 - 5% MAC CG travel is observed within necessarily limits	50
Figure 36 - Songbird Max Takeoff Thrust Required is 124,000 lbf.....	51
Figure 37 - Trend Predicts an Engine TSFC of 0.47 by 2029	52
Figure 38 - Trent 7000 Selected as Propulsion System for Songbird.....	55
Figure 39 - Engine Installation and Anti Ice System	56
Figure 40 - Category IV Gates can Accommodate the Songbird	57
Figure 41 - Songbird Wingtips Encroach 27 ft into Adjacent Spaces.....	58
Figure 42 - Aircraft Wingtips fold 27 ft on each side	58
Figure 43 - NASA (2)-0518 Airfoil.....	59
Figure 44 - NASA (2)-1010 Airfoil.....	59

Figure 45 - NASA (2)-0712 Airfoil (Final Airfoil Selected)	60
Figure 46 - Low-Speed Lift Curves for all Configuration	61
Figure 47 - Lift-to-Drag Ratio vs. Lift Coefficient at Mach = 0.77	62
Figure 48 - Lift Coefficient vs. Drag Coefficient at Mach = 0.77	62
Figure 49 - Takeoff Length is a Balanced Field of 5900 ft	64
Figure 50 - Landing field at Sea Level ISA + 15 °C is 3012 ft	65
Figure 51 - Operational Envelope for Songbird	66
Figure 52 - Payload vs Range Curve	67
Figure 53 - V-n gust diagram at 30,000 ft	68
Figure 54 - Wing Box Structure Configuration	69
Figure 55 - Landing Gear Placement	71
Figure 56 - Architectures' Takeoff Rotation Angle and Clearance	72
Figure 57 - Landing Gear Overturn Angle	72
Figure 58 - Maximum Roll Angle with Angular Clearance	73
Figure 59 - Notch Chart Showing CG Travel	74
Figure 60 - Songbird Control Surface Placement	75
Figure 61 - AVL Model of Songbird	76
Figure 62 - Trefftz Plane Plot of Songbird	77
Figure 63 - AtmosT's Preliminary Manufacturing Concepts	80
Figure 64 - Block Diagram of Flight Control System	81
Figure 65 - Reliability Comparison to Existing Aircraft	82
Figure 66 - CO₂ Emissions vs Average Fuel Burn	84

List of Tables

Table 1 - Compliance Matrix	13
Table 2 - List of the Most Frequently Flown to Airports from ATL & Flight Distances	16
Table 3 - Number of CAT III and CAT IV Aircraft Servicing the Selected Flight Routes .	17
Table 4 - Songbird Key Characteristics	30
Table 5 - Double Eco Key Characteristics	31
Table 6 - Total Cost for Development and Production using Two Methods	33
Table 7 - Breakdown of Direct Operating Cost (in 2029\$)	37
Table 8 - Cost Comparison of Both Architectures and Similar Aircraft.....	38
Table 9 - Weight Fractions for 3500 nmi Mission.....	41
Table 10 - Volume of Fuel Tanks	44
Table 11 - Potential Engine Candidates for HCSR Songbird	53
Table 12 - Scores to Evaluate Propulsion System	53
Table 13 - Trent 1000 and Trent 7000 Are Well Suited for Design Objectives	54
Table 14 - Takeoff Parameters	63
Table 15 - Tire Selection Table	73
Table 16 - Stability Derivatives of Songbird.....	78
Table 17 - Stability Derivatives of Boeing 747.....	78
Table 18 - Reliability Subsystem Breakdown.....	82

1.0 Requirements Overview

The aircraft will enter service in 2029. Technologies and innovations should have justification for being applicable to the entry year. All aircraft parameters and flying qualities will be in line with CFR part 25. The aircraft will have a passenger capacity of 400 in a dual class configuration and accommodate two pilots and eight flight attendants. The range of the aircraft will be 3500 nmi with a design reference mission of 700 nmi. The aircraft will be capable of taking off and landing on a 9000 ft runway and clearing a 35 ft obstacle.

The objective is to offer an aircraft that has enough seating to meet demands and reduce congestion, while also being equal or more economical and safer than other options.

2.0 Compliance Matrix

Table 1 - Compliance Matrix

Requirement	Performance	Comments
Entry into Service of 2029	Meets	
The design range mission is 3,500 nmi with reserve energy to meet 14 CFR Part 25 requirements	Meets	
Capable of taking off and landing from runways (asphalt or concrete)	Meets	
Capable of VFR and IFR flight with an autopilot	Meets	
Capable of flight in known icing conditions	Meets	
Meets applicable certification rules in FAA CFR Part 25 (all missions below assume reserve and equipment required to meet applicable FARs)	Meets	
Engine/propulsion system assumptions documented (Use of engine(s) that will be service by 2029)	Meets	Currently serviced engine: 7000
Crew: 2 pilots, 8 flight attendants	Meets	
Passenger capacity of 400 in dual class configuration	Meets	
50 passengers in Business class with 36" pitch, 21" width	Meets	2-3-2 configuration
350 passengers in Economy class with 32" pitch, 18" width	Meets	3-4-3 configuration
5 cubic feet per passenger baggage	Meets	2,000 cubic feet allotted to store baggage
Galleys, Lavatories, and Exits to meet 14 CFR Part 25	Meets	Three galleys, 8 lavatories, and 8 Type I exits

Number of aisles appropriate to the passenger layout	Meets	Two aisles
Passenger/pilot/attendant weight of 200 lbs	Meets	Total payload weight of 92,000 lbs Total crew weight of 2,300 lbs
Baggage weight per occupant of 30 lbs	Meets	
Maximum takeoff length of 9,000' over a 35' obstacle to a runway with dry pavement (Sea Level ISA +15 degrees C) at MGTOW (Takeoff distance should be calculated to meet 14 CFR Part 25 requirements and be a balanced field length)	Meets	Balanced field length of 5,800 ft
Maximum landing field length of 9,000' to a runway with dry pavement (Sea Level ISA + 15 degrees C) at the end of the design range mission	Meets	
Maximum approach speed of 145 KCAS at the end of the design range mission	Not Met/Tradeable	Approach speed is 161 KCAS at sea level + 15 degrees C
Cabin pressurized to 8,000 ft pressure altitude at maximum flight altitude	Meets	
Minimize operating cost of the aircraft based on a reference mission of 700 nmi	Meets	Cost per seat per mile = \$0.17
Reserve for flight to alternate airport 200 nmi from destination airport	Meets	
Reserve for a 30-minute hold at the alternate airport	Meets	
Reserve for 5% contingency fuel, defined as 5% of non-reserve block fuel	Meets	

3.0 Design Approach

3.1 Mission Marketing Study

While the RFP has identified the problem that we need to solve, as well as the solution to solve it, we felt the need to conduct our own research to further assess the market and determine how effective our aircraft would be.

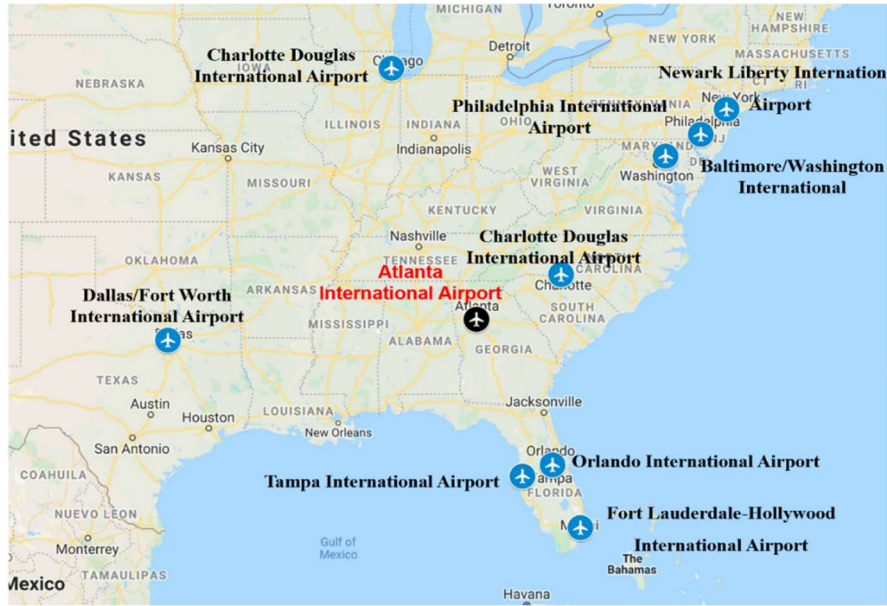


Figure 1 - Most Frequently Flown to Airports Within 700 nmi from ATL

The study consists of closely monitoring major hub airports in both the US and Europe where congestion and delayed flights are noticed. A quick search has identified Atlanta International Airport (ATL) to be one of the largest and busiest airports in the United States, thus, would be an ideal airport that benefit greatly from our short-range high capacity aircraft. To truly find out the magnitude of the congestion issue, the team started researching the most frequent flights routes, the ones that are likely to benefit from our aircraft and would be more likely to fill a 400-passenger aircraft. The team filtered all destinations that are within a 700 nm radius and with a runway of at least 9,000 ft, as suggested by the RFP. **Table 2** indicates the most flown to airports from ATL. According to the team research, as shown in **Table 3**, the number of flights per month from ATL to every one of the listed airports, averaging to about ten flights per day per destination.

Furthermore, the team started looking at flights that occur on an arbitrary selected date, in this case June 1st was selected. The team's goal was to accurately determine the number of flights that occur on a daily basis as well as the number of CAT III and CAT IV aircraft that Songbird

aircraft for each of the previously selected flight destination, leading to reducing the total number of aircraft both on the tarmac and in the sky, on a single day.

Table 2 - List of the Most Frequently Flown to Airports from ATL & Flight Distances

Airport	Number of flights being serviced by CAT III & IV aircrafts/month (from ATL)	Flight Distance nmi
Orlando International Airport	540	351
Fort Lauderdale-Hollywood International Airport	630	506
O'Hare International Airport	360	527
Tampa International Airport	390	354
Baltimore/Washington International Thurgood Marshall Airport	420	501
Charlotte Douglas International Airport	150	197
Newark Liberty International Airport	450	648
Dallas/Fort Worth International Airport	330	634
Philadelphia International Airport	330	579

Table 3 - Number of CAT III and CAT IV Aircraft Servicing the Selected Flight Routes

Airport	Number of CAT III and CAT IV Aircraft before Implementing High Capacity Short Range Aircraft	Number of CAT III and CAT IV Aircraft after Implementing High Capacity Short Range Aircraft
Orlando International Airport	10	8
Fort Lauderdale-Hollywood International Airport	11	9
O'Hare International Airport	7	5
Tampa International Airport	7	5
Baltimore/Washington International Thurgood Marshall Airport	8	6
Charlotte Douglas International Airport	3	1
Newark Liberty International Airport	8	6
Dallas/Fort Worth International Airport	6	4
Philadelphia International Airport	6	4
Total	66	48

Given the team’s finding, and by assuming that two of our High Capacity Short Range aircraft would replace four of the currently used aircraft, a reduction approximated at 27% in the numbers of aircraft on a single day is expected, while still capable of transporting the same number of passengers. The assumption would require total of eighteen of our aircraft to initially break into

the market as it is initially breaking into the market, at a single major hub airport, and will exponentially progress as AtmosT increases its production rate.

Due to the spread of COVID-19, which has led to the cancellation of many flights, the team was not able to accurately assess the need for our aircraft at other major congested airports, but rather, estimated the need based on the team's study on ATL airport. By applying the same percentage of reduction across all major hub airports, the team estimated that total of 180 of the newly designed short range high capacity aircraft, will be utilized and effectively reducing the number of aircraft and alleviating congestion across five major airports in the US and five major airports across Europe, within the first year of production.

3.2 Concept of Operations

As increases in world population create a proportional increase in air travel demand, airport congestion poses a particularly serious safety hazard when it comes to the efficiency of airport capacity and operations. Since airports can only respond so fast to expanding infrastructure to accommodate such a demand, the other viable solution is to design a transport aircraft that will replace today's smaller aircraft to fly short routes (~700 nmi) with increased passenger capacity (~400 passengers). Therefore, the aircraft shall be designed to reduce congestion, which would target the alleviation of aircraft operational activities from aircraft wheels down at the arrival airport to aircraft wheels up.

The first analysis done was to first look at the current gate utilization at some of America's major airports. According to a research study made by MIT, as shown in **Figure 2**, aircraft were observed and organized based on the FAA's CAT system, which organizes the aircraft from smallest to largest wingspan [11].

FAA Aircraft Design Group	Aircraft Type	Minimum Wingspan(ft)	Maximum Wingspan(ft)	Typical Aircraft
I	Small Regional	0	49	Metro
II	Medium Regional	50	79	CRJ
III	Narrow body/ Large Regional	80	118	A320/B737
IV	Wide body	119	171	B767
V	Jumbo	172	214	B747/B777/A330/A340
VI	Super Jumbo	215	262	B747-800/A380

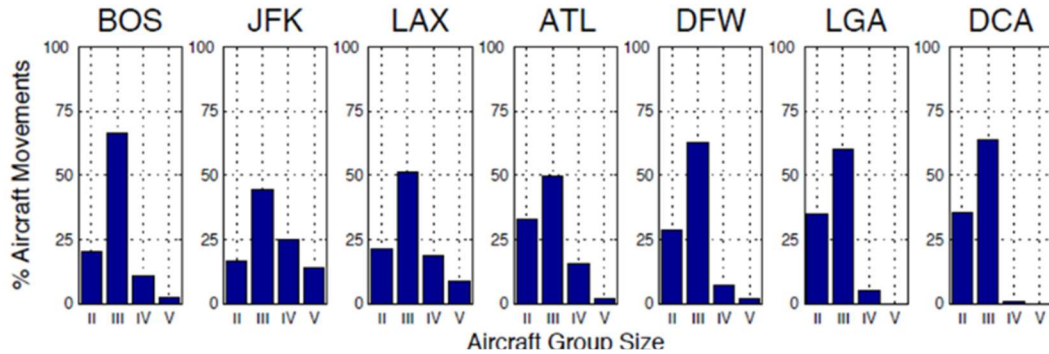


Figure 2 - MIT Research Shows CAT III is the most Utilized Gate Type

Based on this data, CAT III gates (b = 118 feet) are the most utilized gate type at any given time. Since the Boeing 777x has proven that aspect ratio is not physically restrained due to folding wing tips at the gates, one of the ideas that will be explored further is folding wings such that it fits into CAT III gates.

The second analysis employed to analyze ground operations was the use of a custom model-based systems architecture. This approach allows the operational architecture to be crossed with the functional architecture to generate the physical architecture of the aircraft design. Additionally, this gives the team the added benefit of increasing traceability through all the aircraft requirements and mitigate operational hazards. As shown in **Figure 3**, this shows the ViTech CORE 9 operational activity flow diagram of various ground operations at the gate [17].

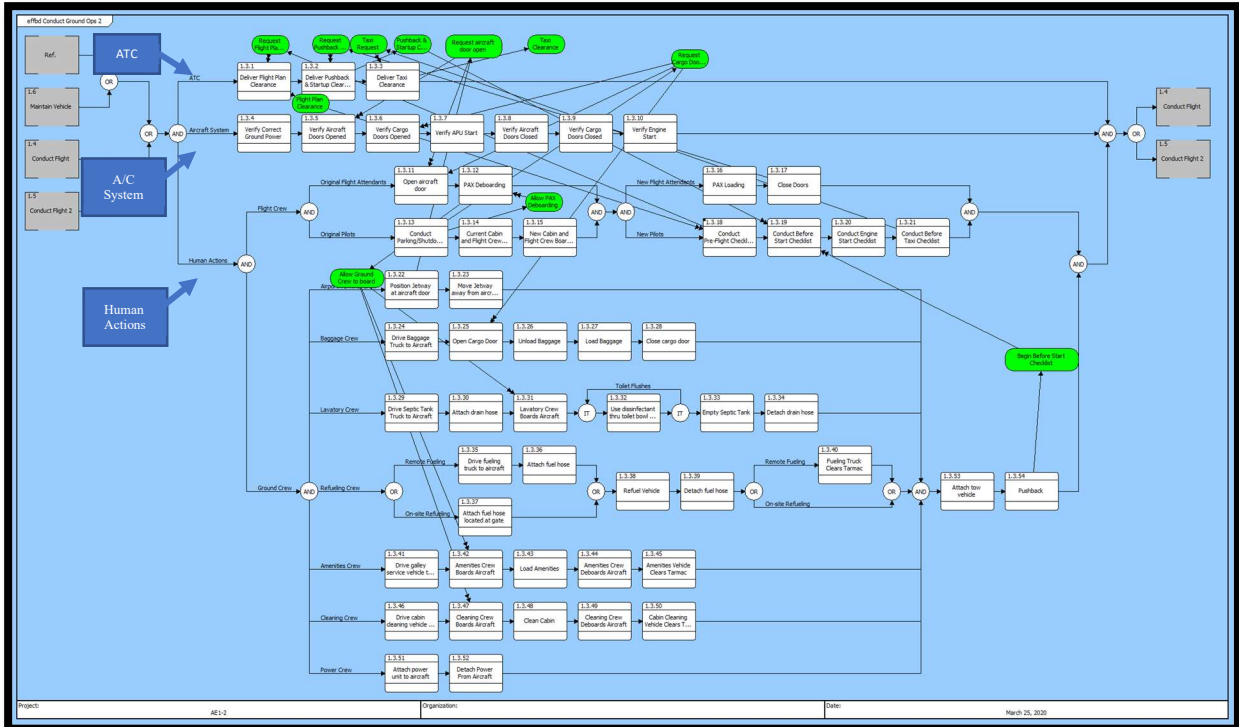


Figure 3 - Model Simulates Turn Time of Operations from Wheels Down to Wheels Up

This operational enhanced functional flow diagram highlights three operational activity “swimlanes”, namely ATC, aircraft systems, and human actions (e.g. pilots, flight attendants, various kinds of ground crew). They are accompanied by green “triggers” to simulate the operational activities more logically. Additionally, one can keep track of the performers, as shown in **Figure 4**, of such activities to see where operations can be further optimized to reduce turn time.

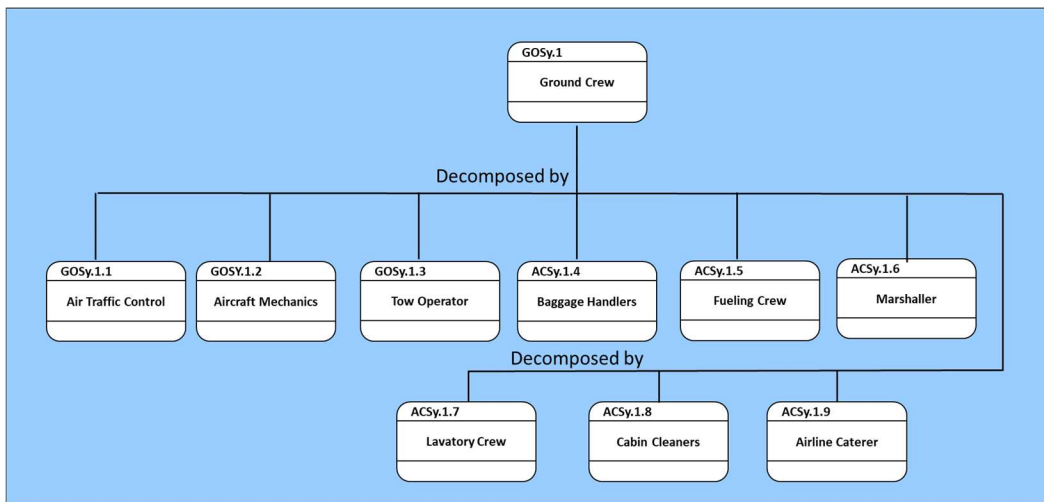


Figure 4 - Decomposition of ground crew personnel

3.3 Mission Profile (3500 and 700 DRM)

The two missions considered was the design range mission of 3,500 nautical miles and the design reference mission of 700 nautical miles. Both missions include a 30 minute loiter and diverting 200 nautical miles to an alternate airport as required per the RFP. The design range mission is shown in **Figure 6** and the design reference mission is shown in **Figure 7**.

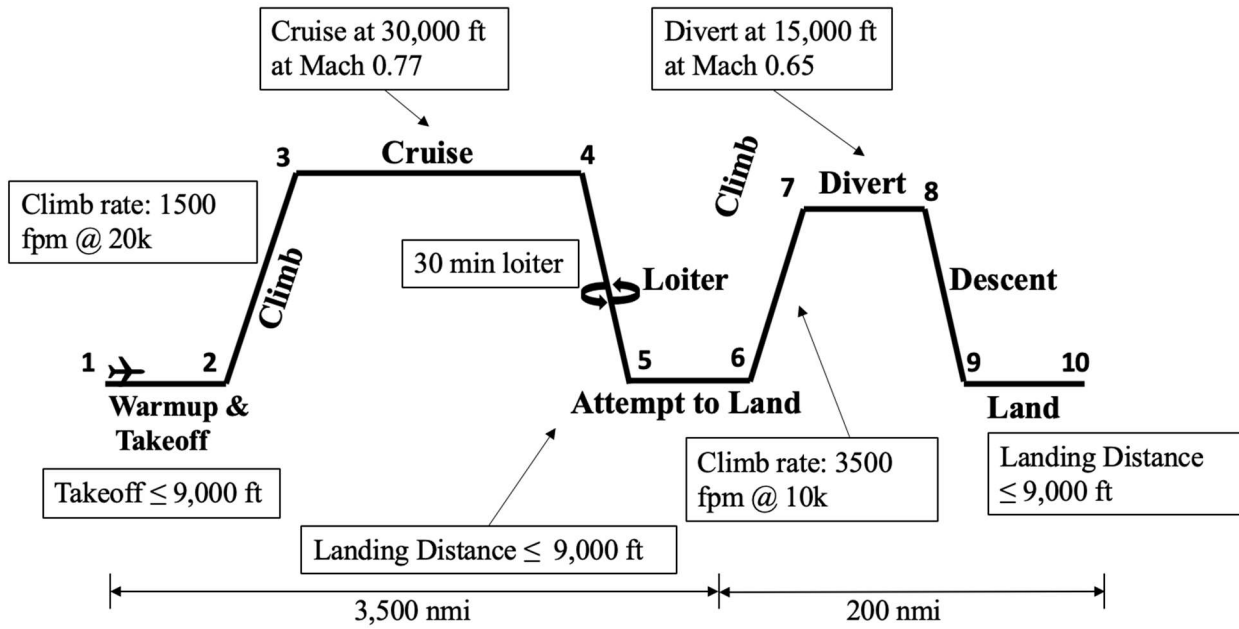


Figure 6 - Design Range Mission

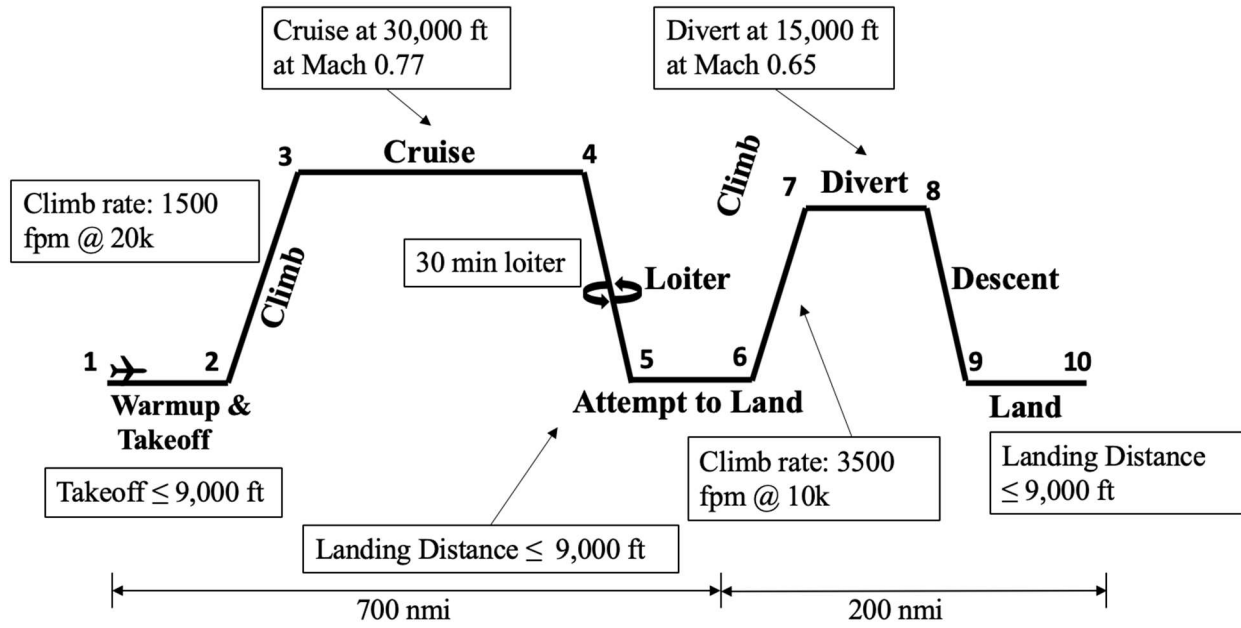


Figure 7 - Design Reference Mission

4.0 Trades of Major Design Components and Final Architecture Selection

This section will go over several newer technologies that could be incorporated into a design of this nature. Innovation is the key to making a design perform than previous versions but needs to be implemented in moderation and with critical analysis on the TRL and feasibility of implementing the technology within the time allowed.

4.1 Side Slip Seats

In section 3.2, it was shown that the critical path that occurs during ground operations for the aircraft include deplaning, cabin cleaning, and enplaning operational activities. Therefore, this necessitated design consideration with respect to the cabin space, namely the seating configuration. This led to the innovative seating configuration known as side slip seating as shown in **Figure 8**.



Figure 8 - Side Slip seating increases aisle width

This side slip seating is an innovative concept because it allows for the aisle seat to actually “slide” atop the middle seat and expand the aisle width as much as 10 inches; keeping in mind that a human is about 16 inches in width standing up.

The pros of this seating configuration are that it enables us to widen aisles at no additional penalty to the aircraft structure, which could reduce turn time during the defined critical path in figure 5. However, since this seating configuration has not been tested yet in a physical setting, the assumption is that the next few years leading to the finalized design will allow the TRL level of the innovation to rise to 9 through the use of enplaning and deplaning simulations.

After applying the side slip seating to the aircraft architecture, **Figure 9** was generated. This graphic shows that an increase in the aisle width due to sideslip seating could lead 35 minutes of turn time savings from landing to takeoff.

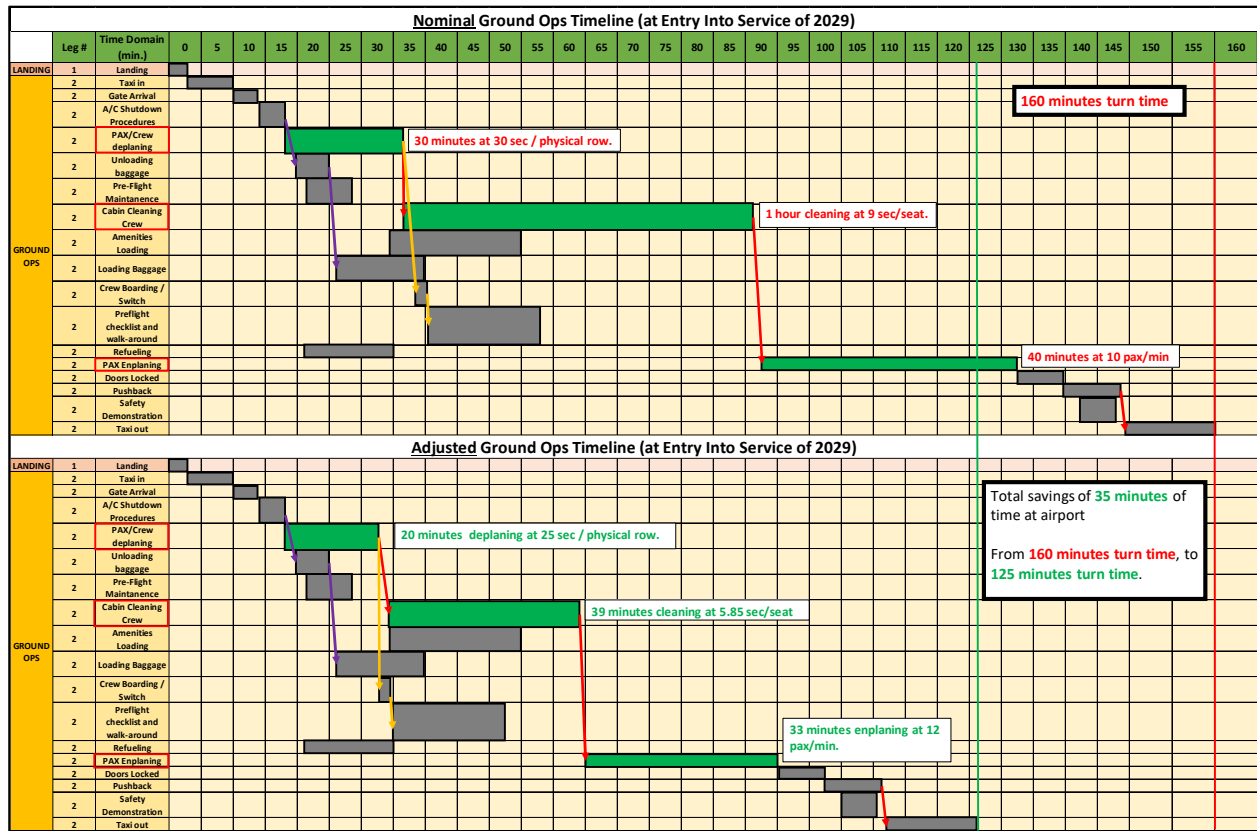


Figure 9 - Songbird can save approximately 35 minutes at the airport

The first operational activity that was adjusted for was the deplaning event. Originally in section 3.2 it was assumed that the mean time for deplaning per row is approximately 30 seconds per row[16]. However, because the target aircraft researched was a Boeing 757, a single aisle, an extra 15 seconds per row were added to account for the extra seats. Accounting now for the wider aisle widths and dual class configuration, we come to an average of about 25 seconds per row for the entire aircraft. Using this calculation, deplaning onto a single gate, single jetway configuration results in a 10 minutes savings.

The second operational activity that was adjusted for was the cabin cleaning event. Here, the main problem that was identified was aisle congestion. Because of the apparent increase in aisle width with the application of side slip seating, there is an opportunity to reduce cleaning time from 9 seconds/seat to approximately 6 seconds/seat for an improvement of 35%. Since the rates assume that we have six crews of 5-6 staff, there is some opportunity to further decrease these

rates as this aircraft becomes a larger part of the market over time. Assuming also a decrease in airliner fleet, then more staff would be available to clean a single aircraft to increase efficiency of cabin cleaning operations, without as many deviations to current operational costs for ground crew.

The third operational activity that was adjusted for was the enplaning event. According to a Boeing trade study, the average rate for a single jetway, single gate loading is approximately ten passengers/minute in 2029. Adjusting this rate from a B757 to the Songbird, the enplaning can be increased from ten passengers/minute to 12 passengers/minute due to the wider aisle seats and double aisle configuration. Conservatively, a savings of seven minutes could be observed. **Figure 10** shows the historical deplaning and enplaning passenger/min rates.

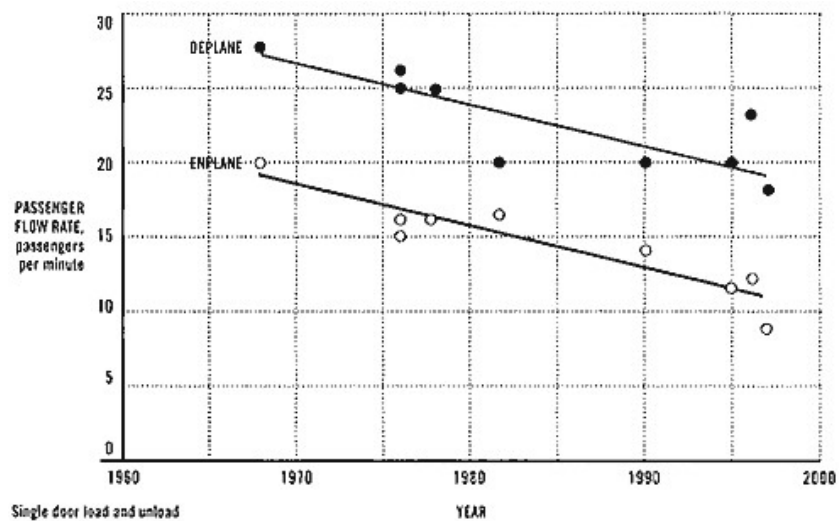


Figure 10 - Historical data trends of enplaning and deplaning on B-757 [16]

4.2 BLI Engine

Boundary layer ingestion (BLI) engines were a possible candidate to enhance the propulsion system. These engines work by taking the unclean air of the boundary layer of the fuselage and accelerating it. According the articles by NASA, a BLI engine could introduce fuel savings of up to 8.5%. Concepts such as the Aurora D8 by Aurora Flight Sciences (**Figure 12**) and the NOVA by Onera (**Figure 11**) are being developed with plans to enter into service by 2030. However, “unclean” air in the engine runs a risk of damaging the blades and causing fatigue much sooner than conventional jets. This along with a low TRL level makes this technology too risky to integrate by the 2029 EIS.



Figure 11 - Onera BLI Aircraft



Figure 12 - Aurora D8 BLI Aircraft

4.3 Strut Braced and Box Wing Designs

Strut braced (**Figure 13**) and box wings (**Figure 14**) both benefit the design by offering a higher L/D ratio. Higher aspect ratios are favorable because they lower the induced drag for the same weight. To support the moment of the wing, a strut is attached from the bottom of the fuselage which increases drag, but still nets a positive decrease in fuel burn. Some articles estimate a fuel savings of 15% and companies such as Boeing are investing into the idea of applying this to class III aircraft. This design has not been implemented on a commercial scale. Furthermore, applying this technology to a 400-passenger aircraft would make the wing too large to fit into any gate without folding the wings significantly.



Figure 13 - Strut Braced Wing



Figure 14 - Boxed Wing Design

4.4 Various Fuselages

Another technology that could be implemented is redesigning the fuselage. Blended wing bodies (**Figure 16**) are seen to have many benefits such as increased fuel and area efficiency. However, a blended wing is only beneficial while it is in the air, so it would not do well on the 700 nmi design reference mission where it must climb and undergo pressurization cycles frequently. Double decker aircraft (**Figure 15**) utilize more of the fuselage cross-section. A double decker would have three aisles and a multiple entry points which would reduce boarding time allowing for more flights/day and less congestion at the terminal. Since the primary mission is to relieve congestion, the double decker was chosen as the second-best architecture to analyze.



Figure 15 - Ecoliner Double Decker



Figure 16 - Boeing BWB

4.5 Configuration/Down Select

The two best candidates for the design were chosen to be a traditional fuselage with side-slip seating (**Figure 17**), and a double decker aircraft (**Figure 18**). These two architectures were analyzed further and values for MTOW, C_d , L/D and DOC were used as measurements on selecting the best architecture. Table 4 and Table 5 show that the traditional architecture performs better than a double decker aircraft. This justified selecting the Songbird for further analysis.

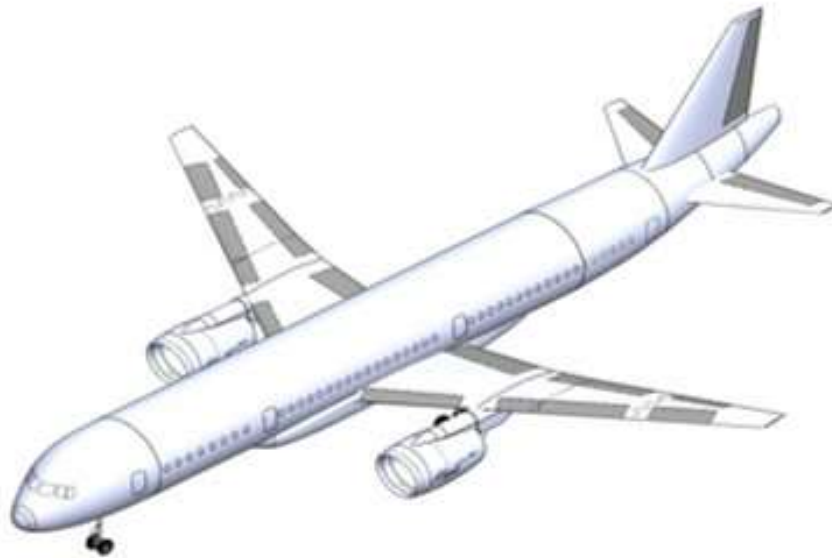


Figure 17 – Songbird

Table 4 - Songbird Key Characteristics

Key Characteristics	
MTOW (lbs)	387,000
L/D at cruise	17.4
C _{DOT}	0.0231
Direct Operating Cost (700 nmi ref mission)	\$45,000

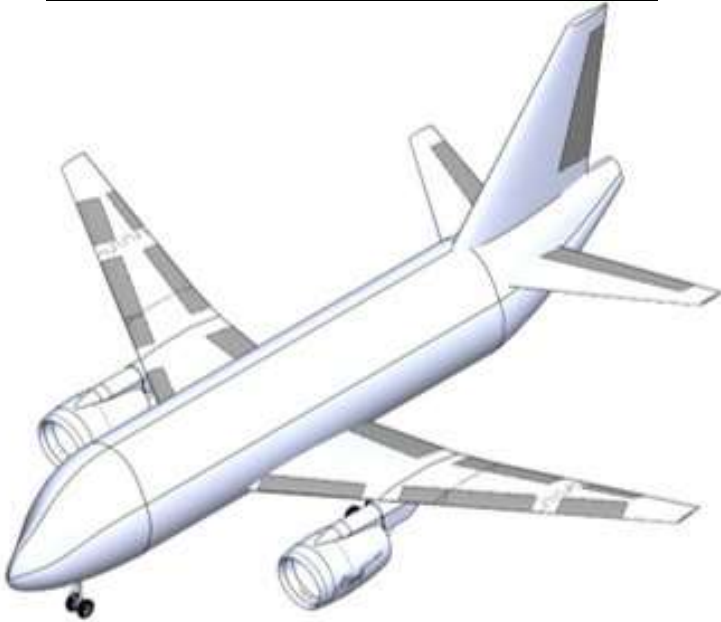


Figure 18 - Double ECO

Table 5 - Double Eco Key Characteristics

Key Characteristics	
MTOW (lbs)	413,000
L/D at cruise	16.5
C_{DTOT}	0.0244
Direct Operating Cost (700 nmi ref mission)	\$49,000

5.0 Cost Estimate

This section will discuss the cost estimates for development, production, and operation. This estimate used equations from Raymer's [5] textbook which were then compared to Nicolai and Carichner's [2] textbook estimates. All cost presented have been adjusted for inflation and are in 2029 dollar.

5.1 Development and Production Cost

The development cost estimate assumes only two aircraft will be manufactured for development, test, and evaluation. The breakdown of each category included in the total development cost is shown in **Figure 19**, where airframe engineering has the greatest cost using both methods.

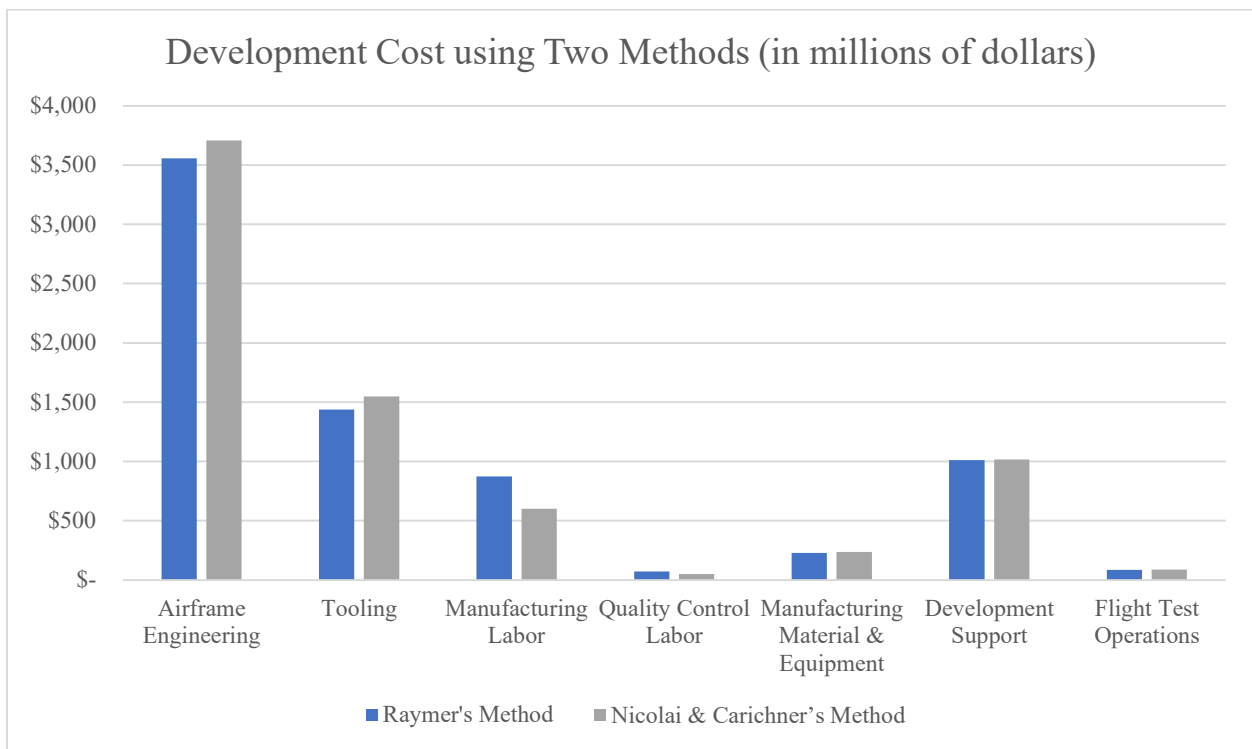


Figure 19 - Breakdown of Development Cost using Two Methods

The production cost estimate assumes a production of 500 aircraft. The breakdown of each category included in the total production cost is shown in **Figure 20**, where the main difference from the two methods comes from manufacturing labor.

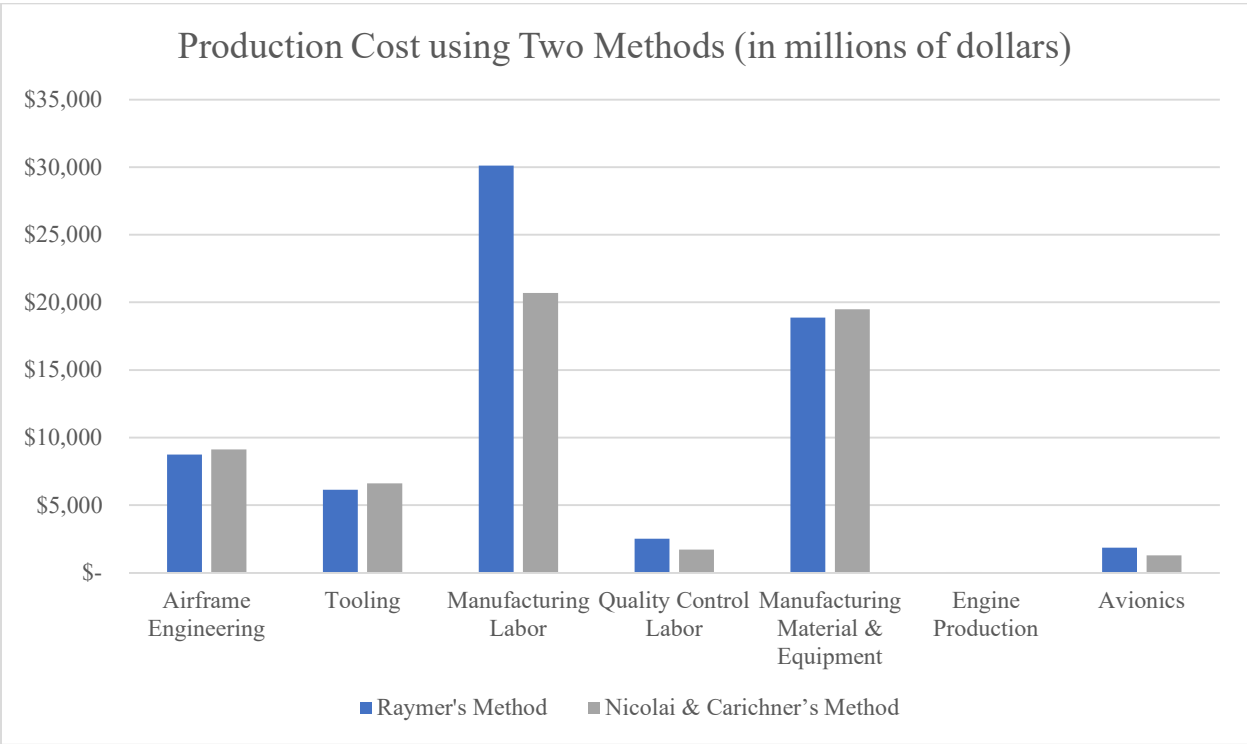


Figure 20 - Breakdown of Production Cost using Two Methods

A summary of the total cost of the development and production phase using the two methods is shown in **Table 6**, where the flyaway cost, cost per aircraft, and price per aircraft at a 15% profit are also included. Raymer’s method yields a more conservative estimate for the cost per aircraft; therefore, this was the method selected for the estimate final estimate.

Table 6 - Total Cost for Development and Production using Two Methods (cost in millions of dollars)

	Raymer's Method		Nicolai & Carichner's Method	
	Development	Production	Development	Production
Total Cost	\$ 7,265 M	\$ 68,325 M	\$ 7,247	\$ 58,981
Flyaway Cost	\$ 137 M		\$ 118 M	
Cost per Aircraft	\$ 151 M		\$ 133 M	
Price per Aircraft (at 15% profit)	\$ 174 M		\$ 153 M	

The plot of production cost vs aircraft sales is shown in **Figure 21** and **Figure 22**, this estimate used the same assumption of a production of 500 aircraft. Using Raymer’s method our breakeven point is at 210 aircraft and using Nicolai and Carichner’s method our breakeven point is at 280 aircraft. The production rate for the aircraft is 15 aircraft per month.

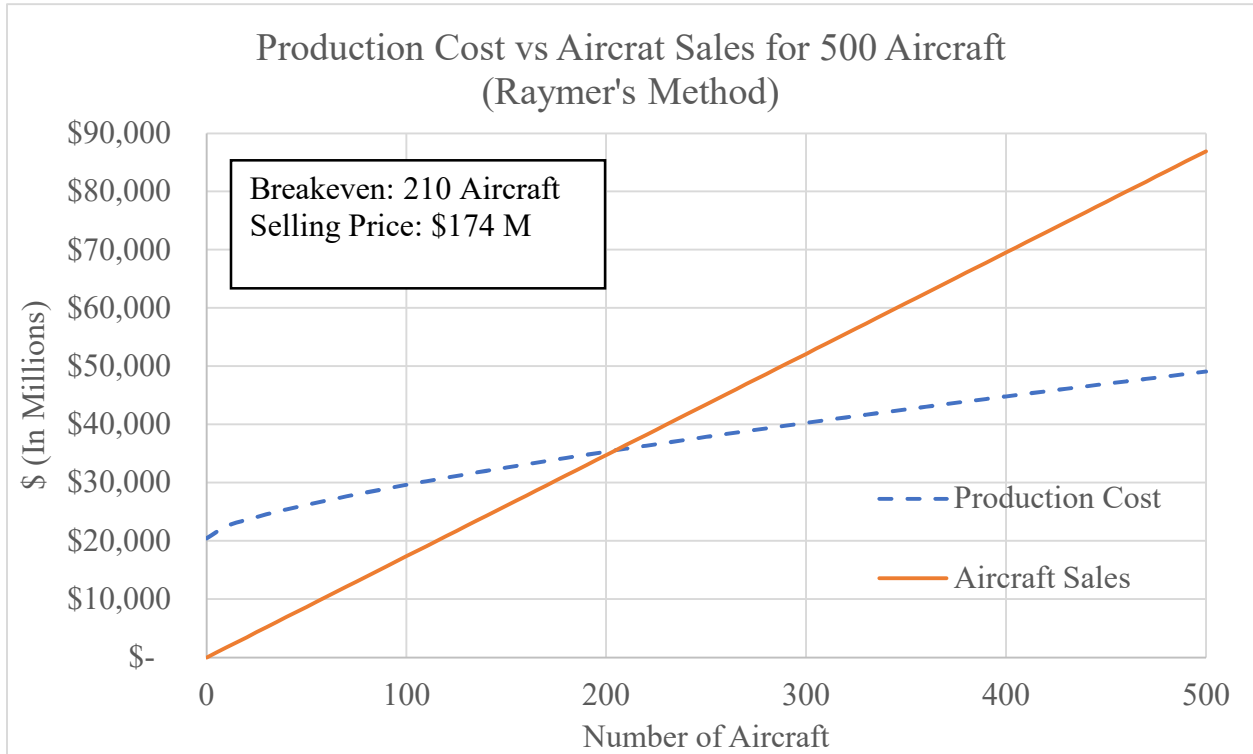


Figure 21 - Breakeven for the Production of 500 Aircraft using Raymer’s Method

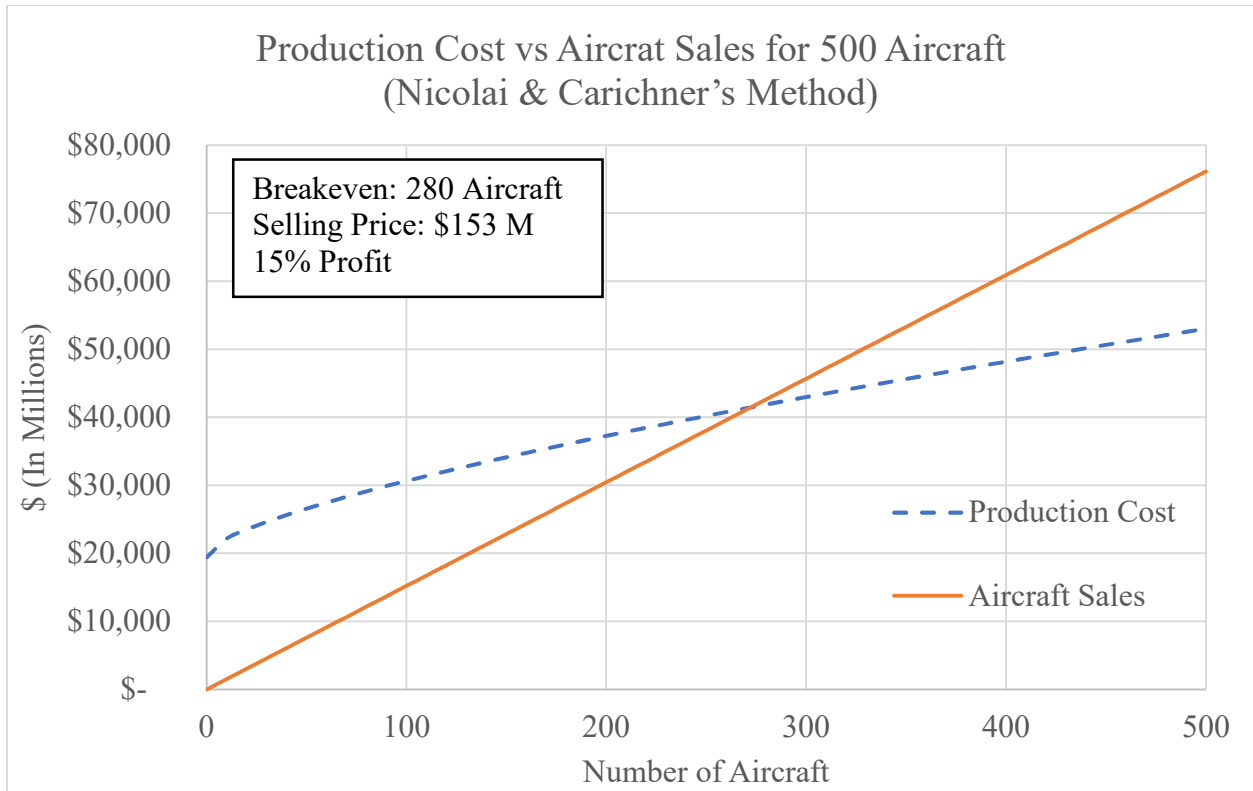


Figure 22 - Breakeven for the Production of 500 Aircraft using Nicolai & Carichner's Method

5.2 Direct Operating Cost

The direct operating cost for the 700 nmi design reference mission was estimated using Raymer's method, and each of the categories consider in the estimate is shown in **Figure 23** and **Table 7**. Fuel is the highest cost of out all the categories, at 40% of the total operating cost. The fuel was estimated using the given price of Jet-A fuel of \$3.00 per gallon + \$3.00 per gallon carbon tax as stated in the RFP.

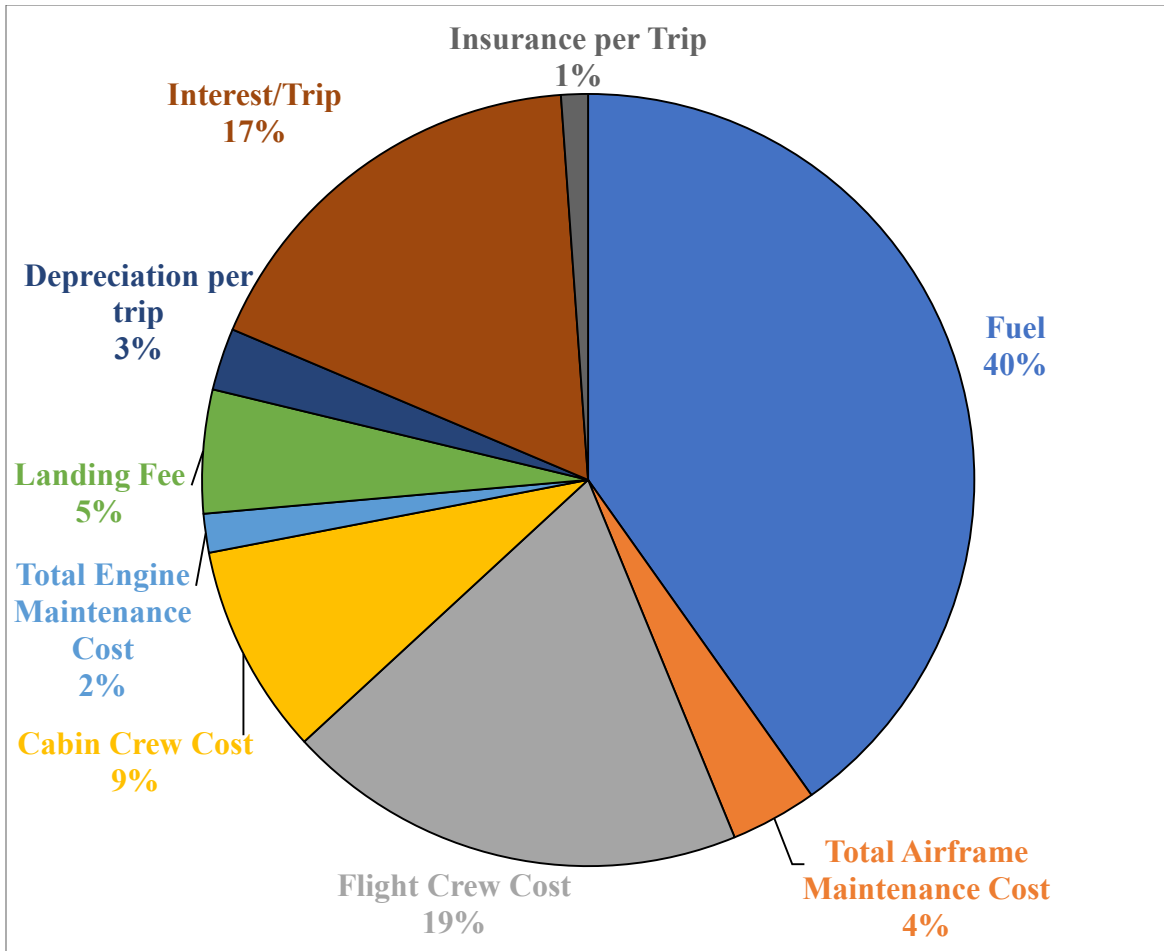


Figure 23 - Breakdown of Direct Operating Cost for 700 nmi Mission

The total direct operating cost for the 700 nmi design mission range was estimated to be \$45,000 per trip, assuming 2,500 trips per year, as well as an airframe life of 20 years and engine life of 15 years.

Table 7 - Breakdown of Direct Operating Cost (in 2029\$)

Category	Cost
Fuel	\$ 17,850
Total Airframe Maintenance Cost	\$ 1,600
Flight Crew Cost	\$ 8,600
Cabin Crew Cost	\$ 3,900
Total Engine Maintenance Cost	\$ 720
Landing Fee	\$ 2,290
Depreciation per trip	\$1,150
Interest/Trip	\$ 7,800
Insurance per Trip	\$ 500
Total Direct Operating Cost	\$45,000

Using this direct operating cost, the estimate cost per seat per mile for the design reference mission was estimated to be \$0.16. The cost of a ticket was estimated to be \$115, with a selling price of \$140 for cash flow to occur after 320 passengers. This ticket price does not assume a different price for the business class, but assuming 35% profit for business seats, the ticket price estimate is approximately \$150 for the design reference mission.

5.3 Cost Estimate Summary and Comparison

The cost estimate summary is shown in **Table 4.3-1**, and it is also compared to similar aircraft such as the Boeing 767 and Boeing 787. The Boeing 767-300 in this comparison is in its maximum arrangement of 351 passengers, and a short-range flight of less than 1,000 nmi was consider. The Boeing 787-8 in this comparison is also in its maximum arrangement of 381 passengers, and a short-range flight of less than 1,000 nmi was consider as well. [8] Overall, architecture 1, Plane Jane has the lowest cost in comparison for the given the design reference mission.

Table 8 - Cost Comparison of Both Architectures and Similar Aircraft

Aircraft	MTOW (lbs)	Passenger Capacity (2 class)	Range (nmi)	cost per seat per mile ('29)	Aircraft Cost (\$ Million '29)	Direct Operating Cost ('29)
Songbird	387,000	400	3,500	\$0.11	\$ 174	\$ 169,000
	300,000	400	700	\$0.16	\$ 174	\$ 45,000
Double Eco	413,000	400	3,500	\$0.12	\$ 181	\$ 173,000
	317,000	400	700	\$0.18	\$ 181	\$ 49,000
Boeing 767-300	350,000	351	<1000	\$0.24	\$ 271	\$ 51,600
Boeing 787-8	502,000	381	<1000	\$0.30	\$ 237	\$ 80,000

6.0 Graphical Representation

6.1 Justification for Diagram (Alt-Mach Trade)

An altitude Mach trade was considered to begin the design process. Altitude and Mach number were traded against fuel burn to find the optimal cruise conditions for the design reference mission of 700 nmi, as shown in **Figure 24**. Fuel burn was traded because it directly correlates to the minimization of the direct operating cost. The trade was performed for the design point of thrust to weight of 0.3, and a wing loading of 120 psf. The chosen cruise conditions are Mach number of 0.77 and an altitude of 30,000 ft.

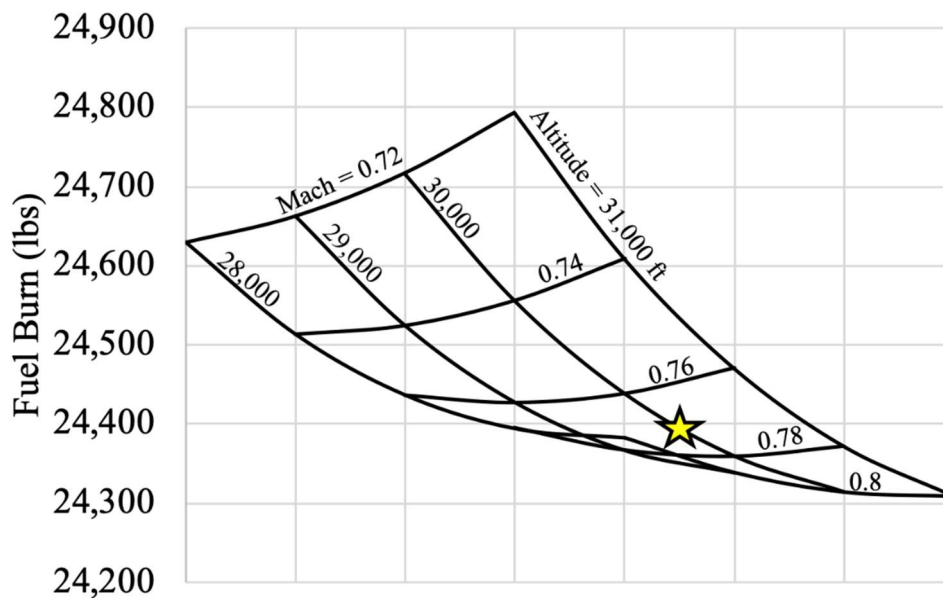


Figure 24 - Altitude-Mach Trade for Optimal Cruise Conditions for 700 nmi

6.2 Design Point (Constraint Diagram)

In finding these values, a constraint diagram was created as shown in **Figure 25**. Requirements for takeoff, landing, and climb rate were plotted with respect to thrust to weight (T/W) and wing loading (W/S) using the constraint equation [22].

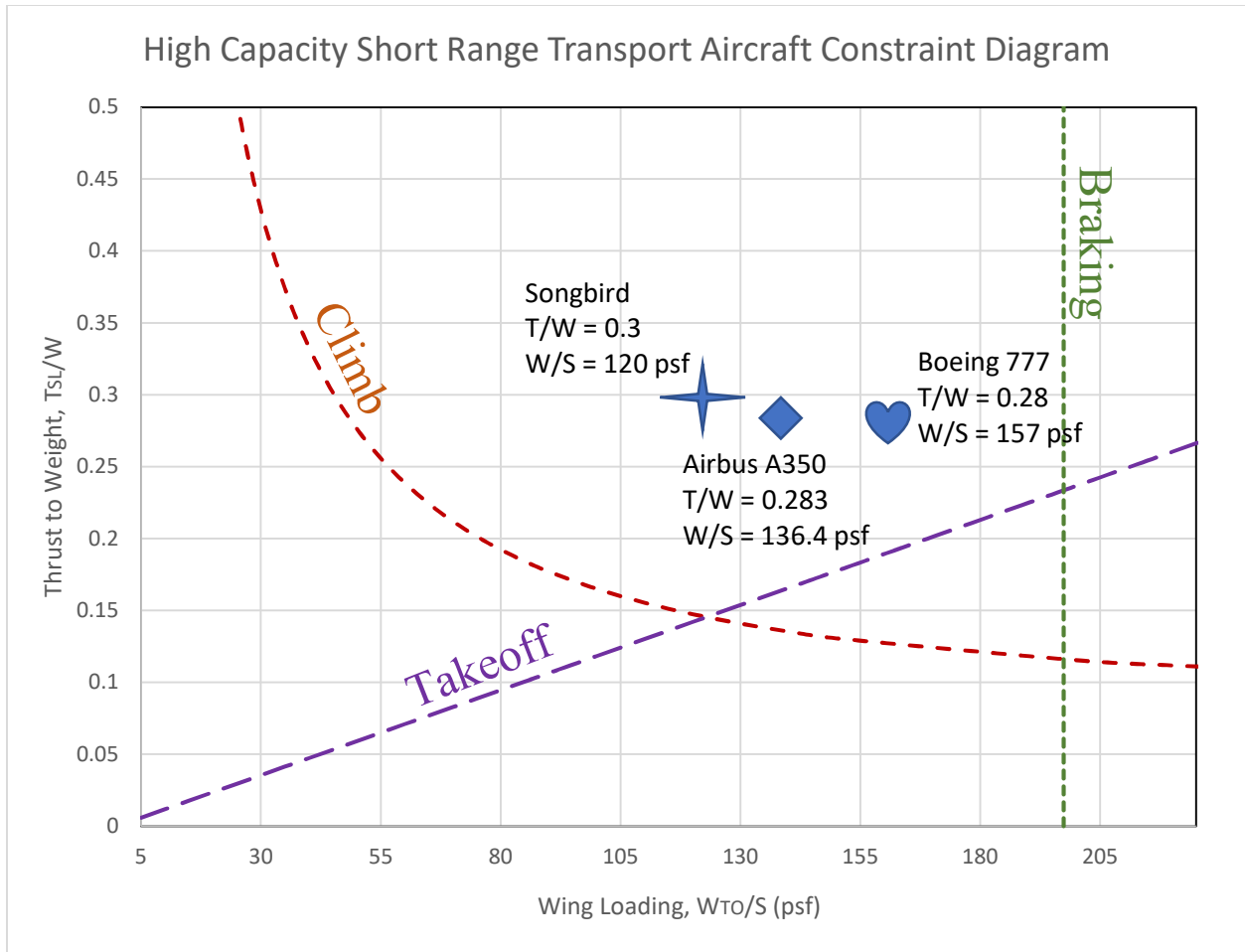


Figure 25 - Constraint Diagram for Aircraft

The results were a thrust to weight of 0.3 and a wing loading of 130 psf. The T/W needs to be multiplied by two to provide sufficient thrust to carry the aircraft in the event of an engine failure. The derived value is shown above compared to aircraft of similar size to verify accuracy. These ratios will be used to find values for thrust and wing area once the maximum takeoff weight (MTOW) is calculated.

6.3 Initial Maximum Takeoff Weight

Obtaining an initial value for weight involved a method shown in Raymer's book. Weight fraction for each mission segment were estimated for the 3500 nmi mission as shown in **Table 9**. The cruise fraction was calculated using the Breguet Range Equation, while figures and historical data yielded the others. Once these values were obtained, the data was plotted against an equation for jets to find the intersection. This method resulted in an initial maximum takeoff weight of

393,000 lbs. A 5% increase was added to account for design growth, making the weight used for sizing the aircraft 412,000 lbs. With this weight and the previous T/W and W/S the thrust and wing area values are calculated to be 124,000 lbf and 3174 ft², respectively.

Table 9 - Weight Fractions for 3500 nmi Mission

Design Ref. Mission #	Weight Fraction	Description	Value	Distance
1	W2/W1	Warmup / Takeoff	0.975	3500 nmi
2	W3/W2	Climb 1	0.985	
3	W4/W3	Cruise 1	0.786	
4	W5/W4	Descent	1	
5	W6/W5	Loiter 1	0.988	
6	W7/W6	Climb 2	0.985	200 nmi
7	W8/W7	Cruise 2	0.984	
8	W9/W8	Loiter 2	0.988	
9	W10/W9	Descent	1	
10	W11/W10	Land	0.995	
1 to 10	W11/W1	Design Reference	0.711	3700 nmi

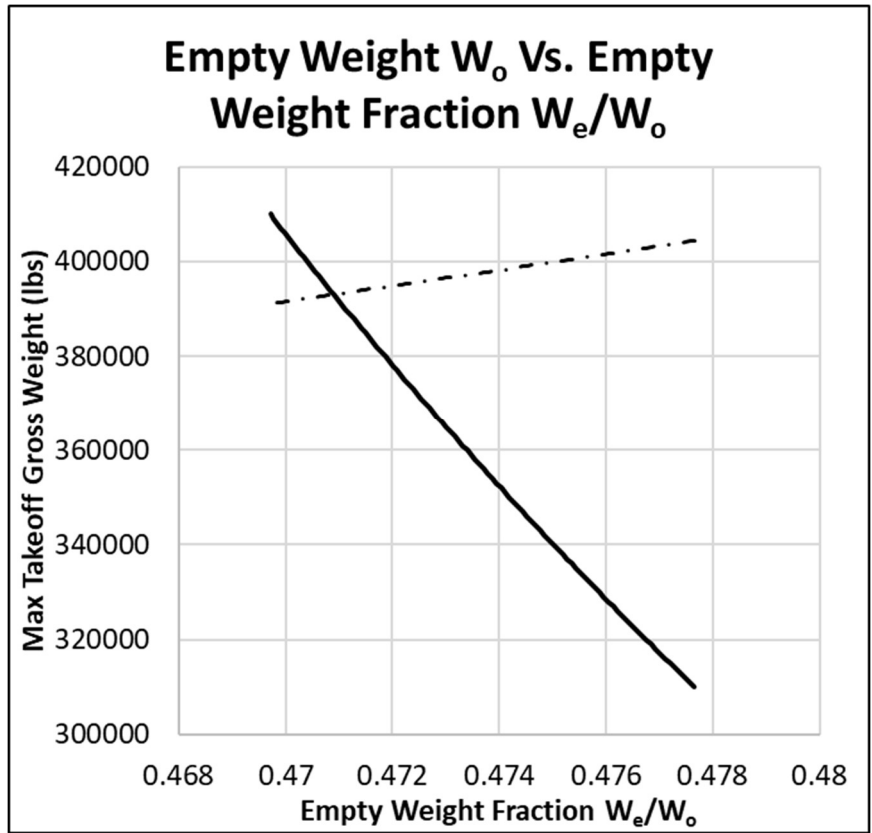


Figure 26 - Empty Weight vs. Empty Weight Fraction

7.0 Geometric Drawings

7.1 Scaled 3-View

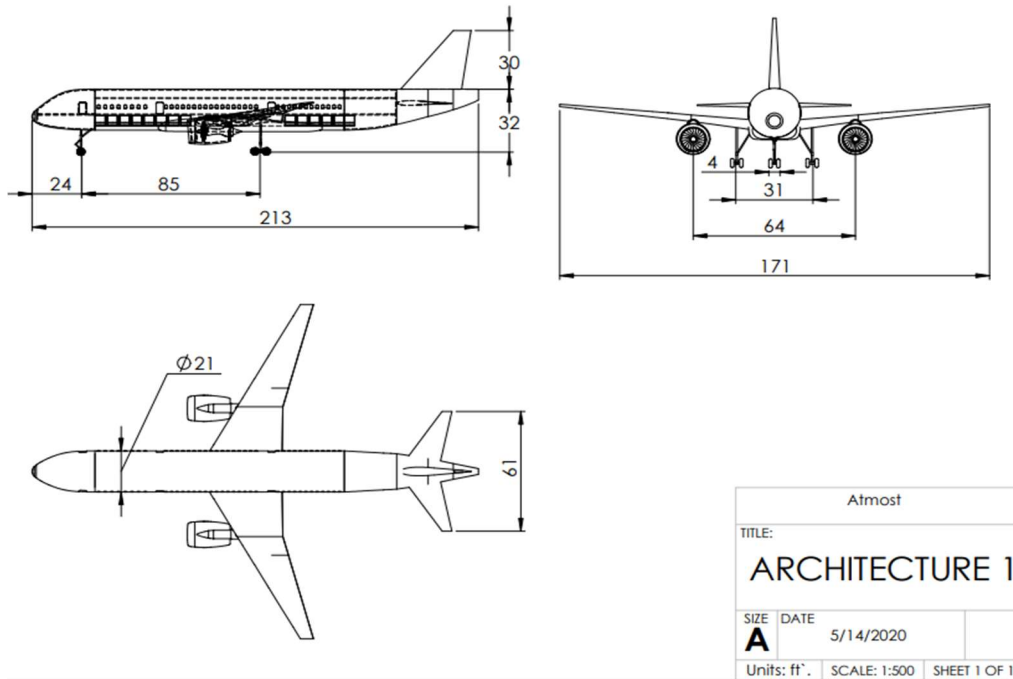


Figure 27 – 3-View of AtmosT Down Selected Aircraft

Figure 27 shows 3-view picture of AtmosT ‘s down selected architecture, showing fuselage length of 213 ft, a wingspan of 171 ft, with a fuselage diameter of 21 ft. The following sections go over fuel tank volume, internal layout, and cross-sectional view.

7.2 Internal Volume Requirements

7.2.1 Fuel Tank

Fuel volume was estimated and calculated to be 1,602 cubic feet at the worst-case scenario and fuel density of 1.5 slugs/cubic feet. Fuel tanks are to be housed within the wing and placed as shown in **Figure 28**.

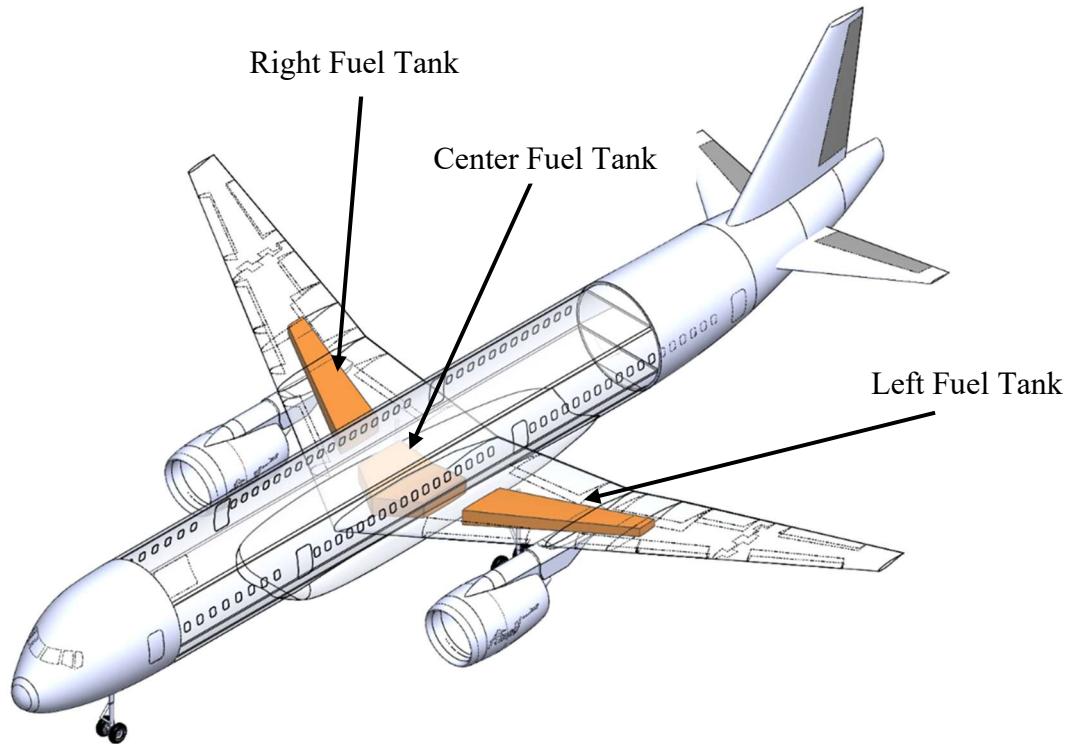


Figure 28 - Placement of Fuel Tanks

Table 10 indicates the fuel tanks and corresponding available volume which has been calculated using SolidWorks, revealing an available volume of 1645 cubic feet.

Table 10 - Volume of Fuel Tanks

Fuel Tanks	Volume (ft ³)
Right Fuel Tank	450
Left Fuel Tank	450
Center Tank	745
Total Available Volume	1645
Required Fuel Volume	1602

7.2.2 Cargo Container

Figure 29 demonstrate the location of both forward and aft cargo door, which have been sized to accommodate for faster loading and unloading of LD-3 containers. **Figure 29** also shows the available cargo volume, and while only 14 LD-3 containers are required to accommodate for the storage capacity needed for passengers and crew members, 28 LD-3 containers can be fitted,

allowing for extra cargo to be carried in case aircraft isn't completely full. **Figure 30** shows a 3D model of LD-3 Containers.

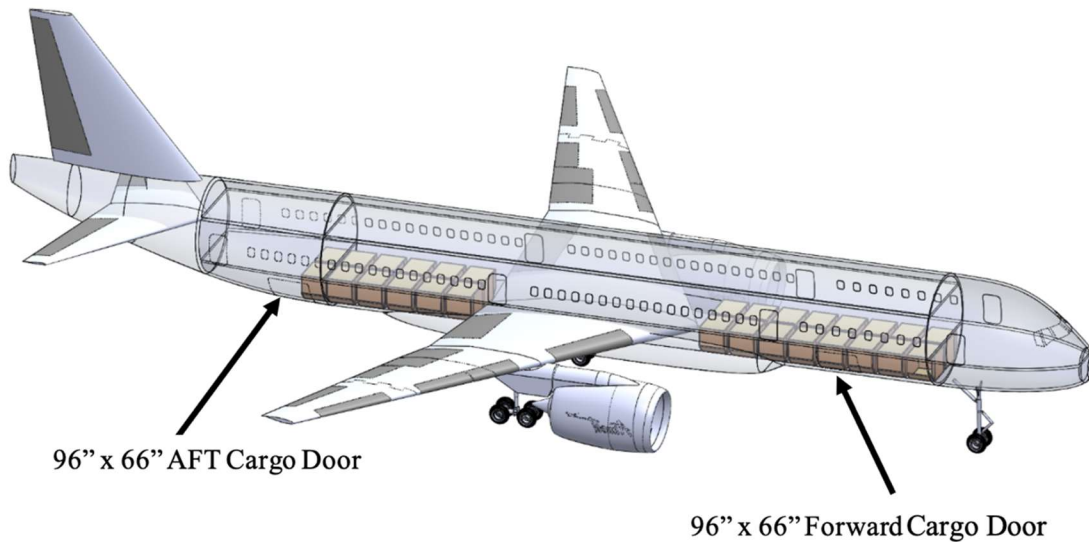


Figure 29 - Cargo Container

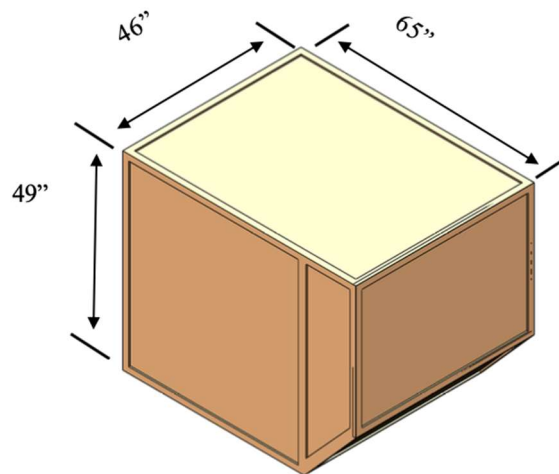


Figure 30 - Dimensions LD-3 Containers

7.3 Cross-section showing passenger seats Layout of passenger

Figure 31 indicates top view of the layout of passenger and amenities in a dual class configuration, featuring a 3-4-3 seating configuration in economy class, and a 2-3-2 seating configuration in business class. Lavatories, galleys, exit doors, and jump seats are shown in according to legends below. **Figure 31** also shows a cross-sectional view of the fuselage featuring

aisle width of 22” while showing a 5’10” passenger and demonstrating the benefit of having slide-slip seats that would effectively increase the width of aisle by 80%, allowing passengers to board the aircraft much faster.

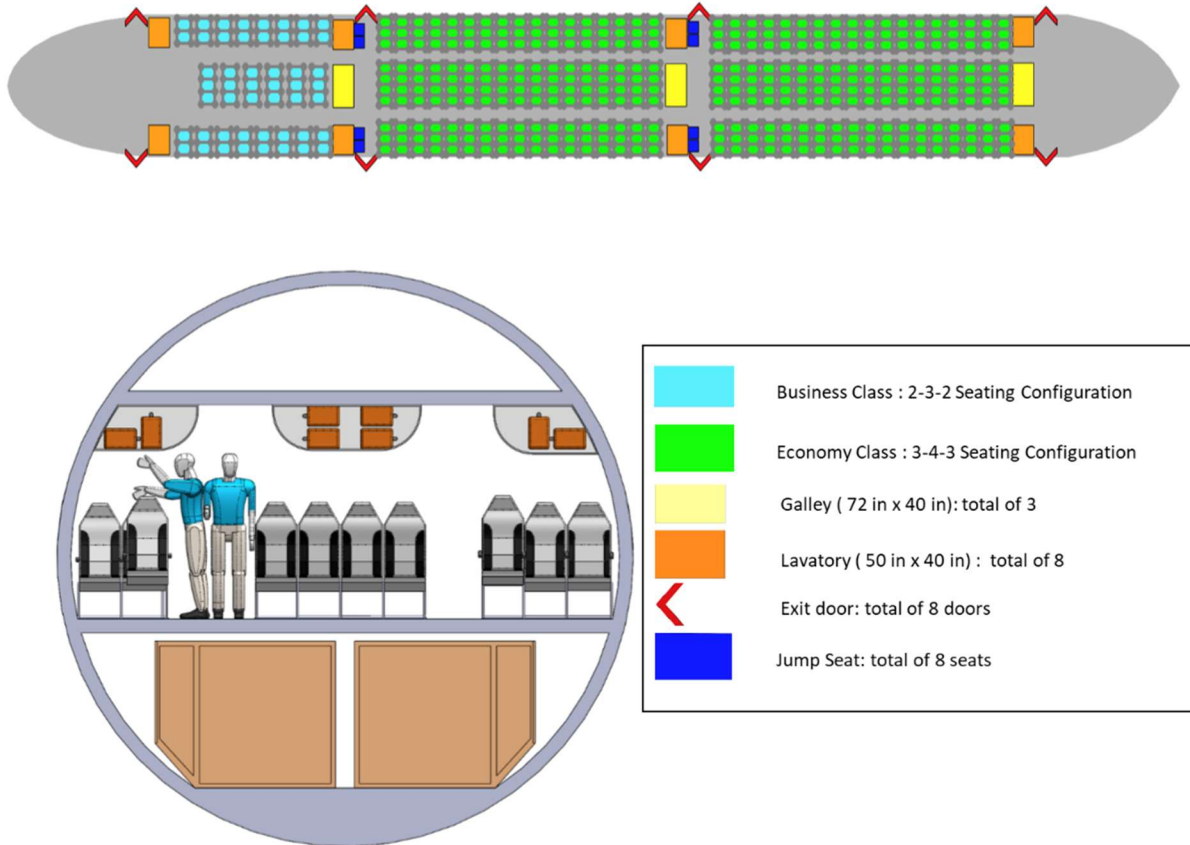


Figure 31 – Layout of Passengers and Amenities

7.4 Layout of Cockpit

Figure 32 shows the layout of the A330 aircraft which is expected to influence the team’s future layout design.

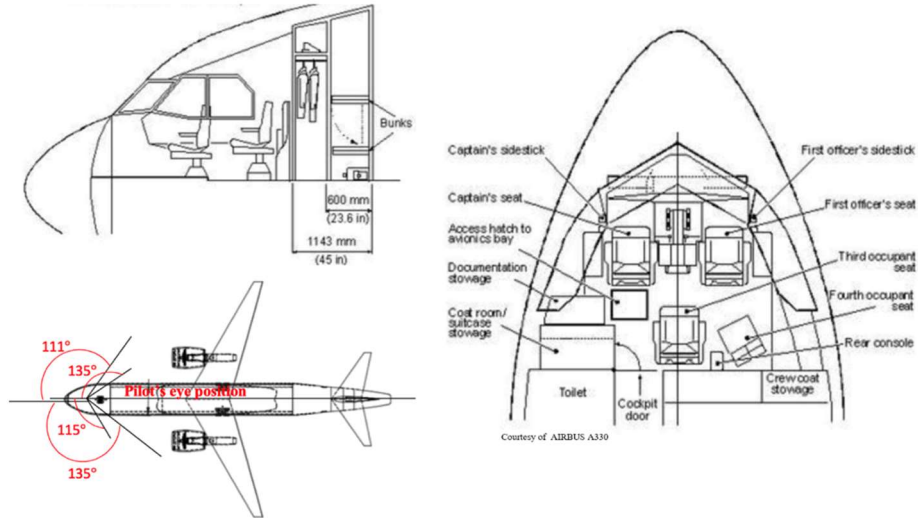


Figure 32 - Cockpit Layout of the A330

7.5 Fuselage centerline diagram

Figure 33 shows the location of static margin, located at, as well as the Neutral point and C.G. location.

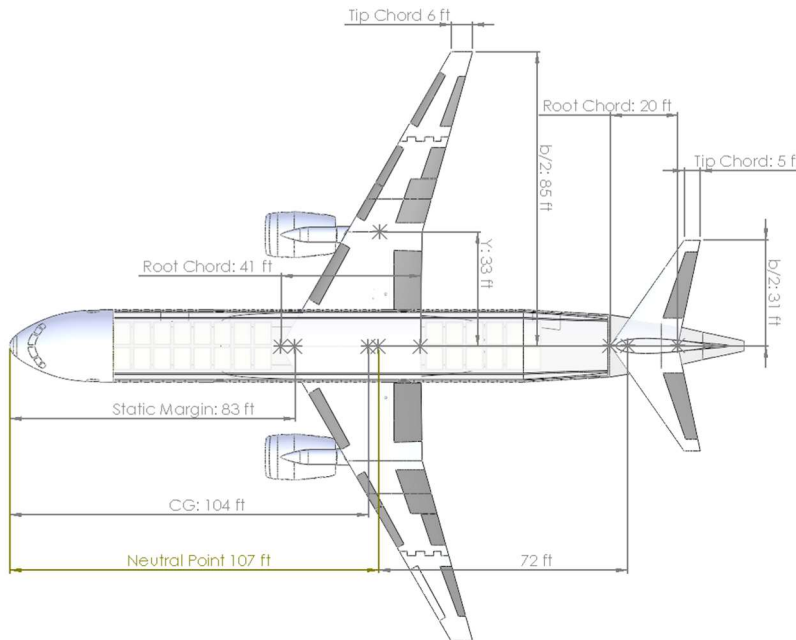


Figure 33 – Aircraft Centerline Diagram

8.0 Aircraft Weight Statement

8.1 Weight Breakdown

As was stated in section 5.3, an impersonal iterative weight statement method derived from Raymer's was used to determine the initial MGTOW of 389,000 lbs. Once more data about the geometries of the aircraft were determined, a refined weight statement method developed by Nicolai and Carichner was utilized.

To better understand Nicolai and Carichner's weight statement method, it is also prudent to list the overall assumptions the authors defined. Some assumptions about the calculations are that it is an "empirical formulation that are conditioned upon the many different geometric properties of the components." [2] Additionally, because the aircraft follows a fairly conventional widebody architecture, with the exception of its folding wing structure and aircraft structure material selection, the equations may be used without any alterations. It is also worth noting that further analysis of the exact composites and foldable wing technologies will need to be done to obtain more accurate weight numbers. This value gives the team an additional value to reference with respect to the initial MGTOW estimate using Raymer's Method.

Additionally, it is important to also define fuel weight estimations as well. The fuel density chosen was at 100 degrees Celsius at approximately 1.5 slugs per cubic feet [9]. Based on the initial weight estimate of 389,000 lbs, it was therefore determined that maximum fuel volume capacity needed was initially 107,000 lbs. However, because this value is based on empirical weight equations and was later found to be an overestimate, based on section 11.4 regarding payload range, the aircraft is designed conservatively. The result was that the fuel requirement will decrease by approximately 30% to a value of 70,000 lbs. This decreased fuel weight defined in section 11.4 will then allow the fuel tank volume to decrease accordingly, having the effect of decreasing the overall MGTOW of the aircraft.

The last contribution to this weight statement is the main system powerplant. The weight of the pair of Trent 7000 high bypass turbine engines mounted under the wing totals to approximately 28,400 lbs [10].

Therefore, the total refined weight statement is approximately 386,000 lbs, which is a difference of less than one percent in weight from the original MGTOW estimate of 389,000 lbs.

The empty weight of approximately 190,000 lbs is shown in **Figure 34**, breaking down the weight into its respective group of components.

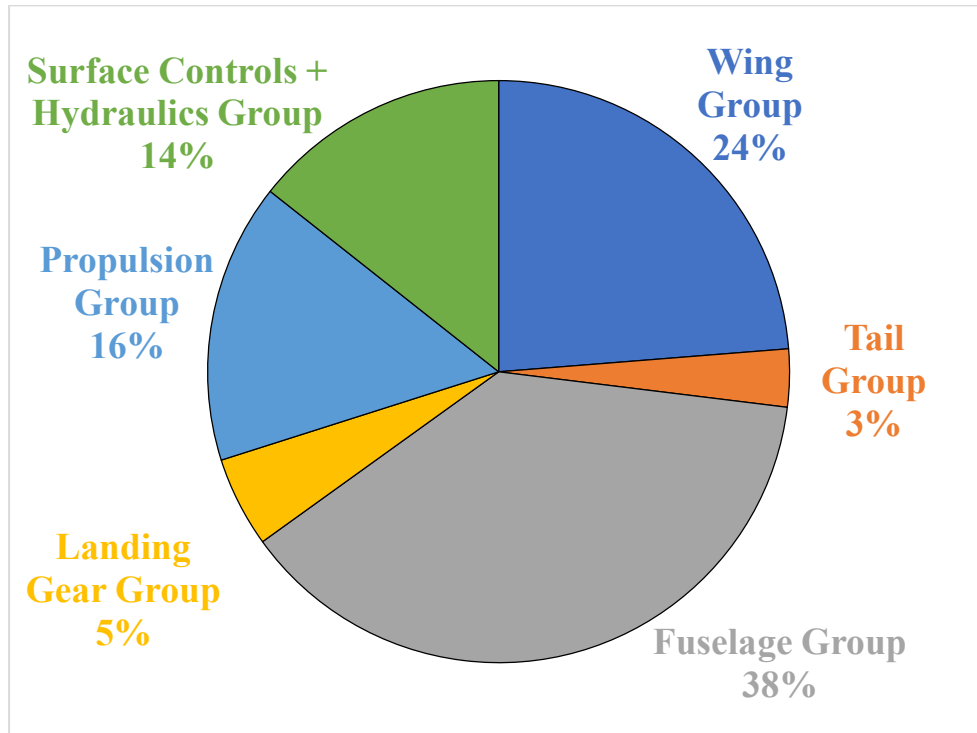


Figure 34 - Fuselage group accounts for ~38% of the calculated refined empty weight

8.2 CG travel using the CG boundaries as defined in the notch chart

Additionally, from this refined weight statement in the previous section, two loading modes were also analyzed for the purposes of ensuring that the aircraft is within its proper CG limits, namely the landing flare and rear stability limits; more information regarding the determination of these limits are also found in 14.1 with regards to the notch chart.

The first mode that was analyzed was boarding the payload first and then the fuel second. The second mode analyzed was fueling the aircraft first, then the payload. Considering the various loading conditions described, **Figure 35** was generated to show the CG travel with respect to the landing flare and the rear stability limit.

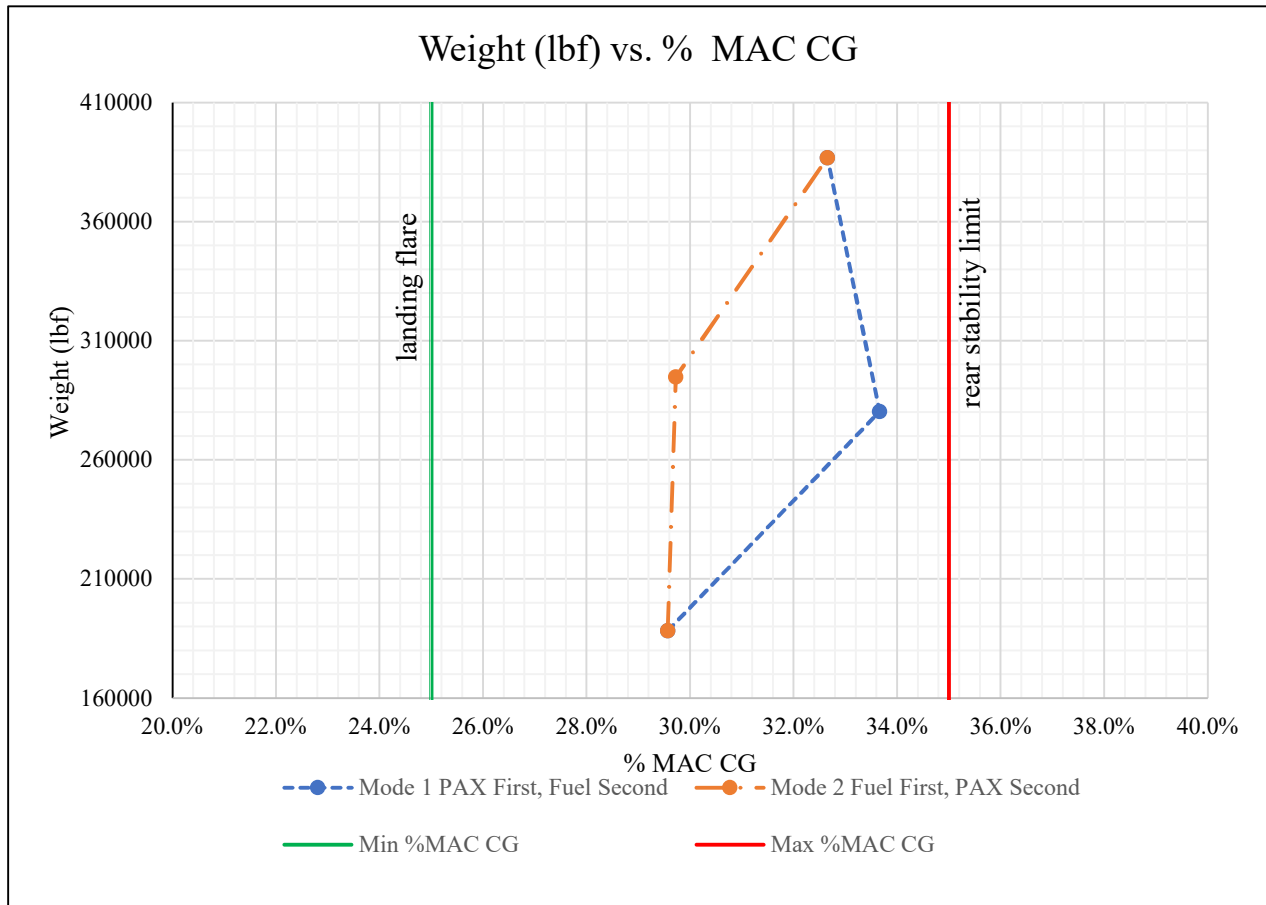


Figure 35 - 5% MAC CG travel is observed within necessarily limits

With at least 4% of allowable CG travel with respect to the upper and lower limits of the aircraft, the aircraft may be assumed to have proper balance as a result.

9.0 Propulsion System

9.1 Propulsion Trade Study

The selection of the propulsion system is based on the preliminary takeoff weight of 412,000 lbs and a thrust to weight ratio of 0.3, which is taken from the constraint diagram. The required thrust for takeoff is calculated to be 124,000 lbf. To select the propulsion system that would meet the takeoff requirements, a trade study of different turbofan configurations was conducted as shown below in **Figure 36**. Turboprops were not included in the study because they are not as efficient at the altitude and Mach number specified by the constraint diagram.

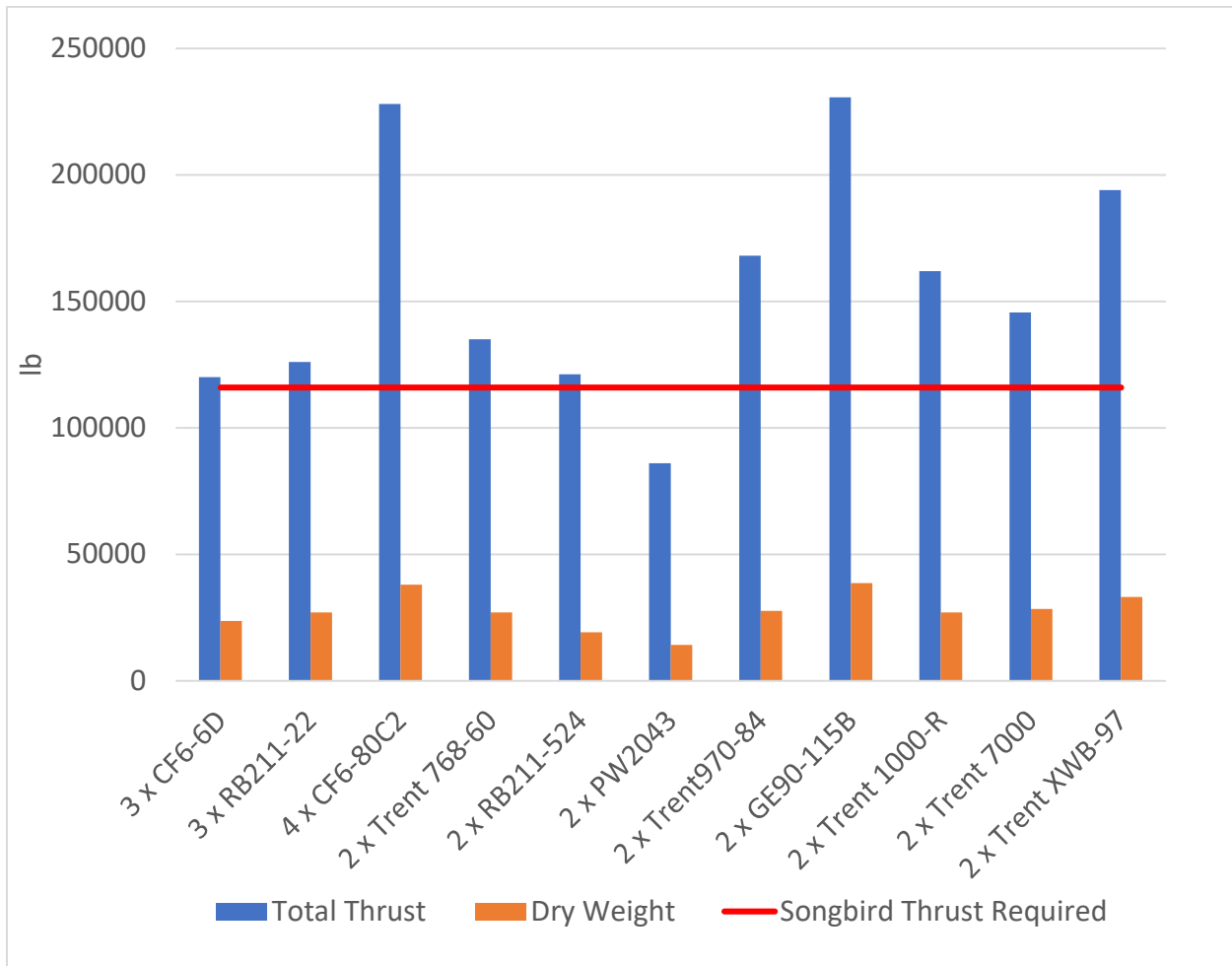


Figure 36 - Songbird Max Takeoff Thrust Required is 124,000 lbf

The RFP required the aircraft to have entry into service by 2029 with minimal operating costs when compared to other similarly sized aircrafts. Thrust specific fuel consumption is an important parameter that can help minimize the operating costs of the aircraft, but engine manufacturers are always seeking ways to improve specific fuel consumptions, and it is uncertain how efficient those engines will be by the time the Songbird enters service. Therefore, the thrust specific fuel consumptions of various turbofans were extrapolated to 2029 to determine an ideal engine TSFC that would be available on future turbofans. As shown below in **Figure 37**, an engine with a TSFC of 0.47 lb_m/hr/lb_f should be available by 2029 if the current trends stay on course. However, the propulsion system of the Songbird will have to be picked from current engines in the market, but their specific fuel consumption will be traded against future engines for the Songbird to stay competitive when it enters service.

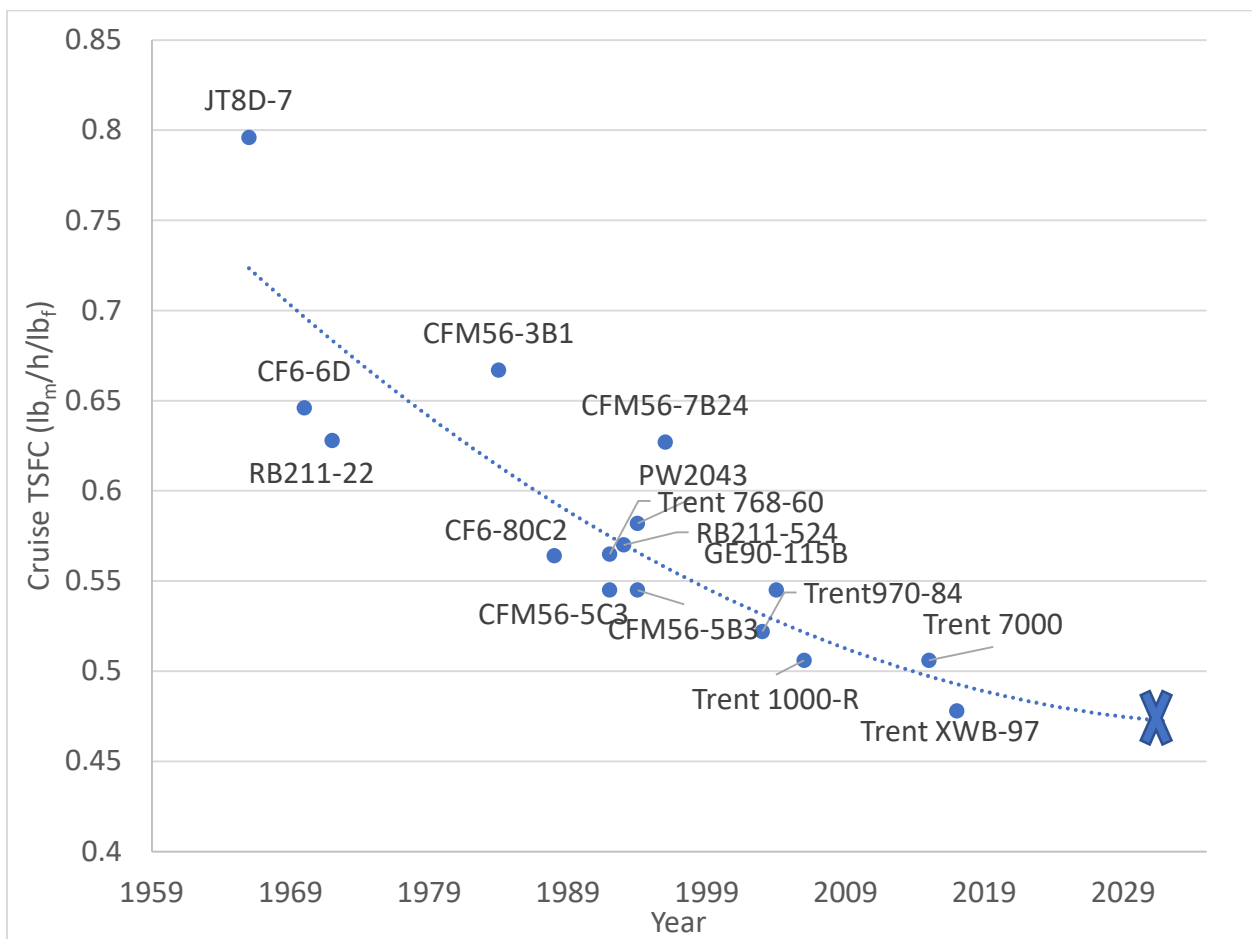


Figure 37 - Trend Predicts an Engine TSFC of 0.47 by 2029

Potential engine candidates that met the threshold for takeoff were compared and tabulated below in **Table 11**. Three and four engine configurations, as well as engines that are no longer in production, are omitted to stay with current market trends and maximize efficiency.

Table 11 - Potential Engine Candidates for Songbird

Engine	TSFC Cruise (lbm/hr/lb _f)	Total Takeoff Thrust (lb _f)	Total Dry Weight (lb _m)	Cost (29' Millions)
2 x Trent970-84	0.522	168000	27600	44.65
2 x Trent 1000-R	0.506	162000	27000	62.86
2 x Trent 7000	0.506	145600	28400	60.07
2 x Trent XWB-97	0.478	194000	33200	68.51

Engine SFC, takeoff thrust, engine dry weight, and engine cost, will determine the engine that will be best suited to accomplish the design objectives of the Songbird. The engine will be scored based on how well it meets the criteria shown below in **Table 12**.

Table 12 - Scores to Evaluate Propulsion System

	9 Extremely suited for Mission	6 Meets baseline requirement	3 Has value but not recommended	0 Does not meet the requirement
Engine Thrust (lb _f)	> 140000	124000 - 140000	12399 - 80000	< 80000 > 165000
Engine Weight (lb _m)	< 30000	30000 - 35000	35001 - 39999	> 40000
Engine Cruise SFC (lb _m /h/lb _f)	< 0.47	0.47 - 0.51	0.51 - 0.55	> 0.55
Engine Cost (2029 \$M)	<55	55-65	66 - 70	> 70

Due to the importance of minimizing operating costs, engine weight and SFC had a higher weight factor in this study. It was determined that the Trent 1000 and the Trent 7000 are the engines that would be best suited to meet the objectives of the Songbird, as shown below in **Table 13**.

Table 13 - Trent 1000 and Trent 7000 Are Well Suited for Design Objectives

		Trent 970-84		Trent 1000-R		Trent 7000		Trent XWB-97	
Criteria	Weight Factor	Score	Weighted Score	Score	Weighted Score	Score	Weighted Score	Score	Weighted Score
Thrust	1	9	9	9	9	9	9	9	9
Weight	2	9	18	9	18	9	18	6	12
SFC	3	3	9	6	18	6	18	6	18
Cost	1	9	9	6	6	6	6	3	3
Total			45		51		51		42

9.2 Final Engine Selection and Justification

The Trent 7000, shown in **Figure 38**, was selected over the Trent 1000 because it is the successor to the 1000 and would have better manufacturer support since it is newer. Although the SFC of this engine has not reached the projected value of $0.47 \text{ lb}_m/\text{hr}/\text{lb}_f$, it is still one of the most efficient turbofans in the current market today. The Trent XWB has a better engine SFC, but it is overpowered for the mission segment, heavier, and more expensive than the other turbofans in the study.

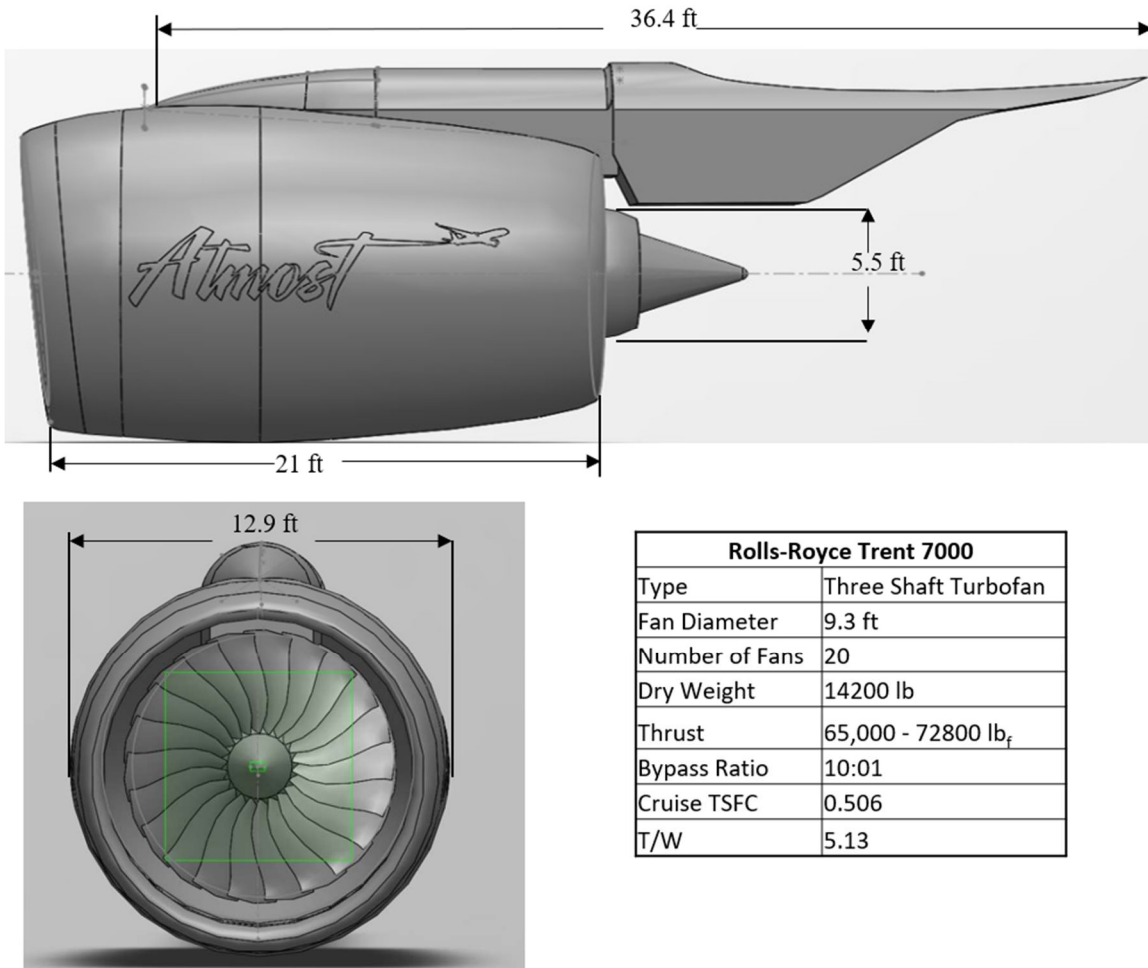


Figure 38 - Trent 7000 Selected as Propulsion System for Songbird

Two Trent 7000 engines would be installed on the aircraft as shown below in **Figure 39**. Based on the requirement of flying in known icing conditions, the aircraft will utilize the bleed air system to prevent ice buildup on the leading edge of the wing. Hot air from the engine bleed valve will be diverted and distributed via ducts along the leading edge of the wing to melt any ice.

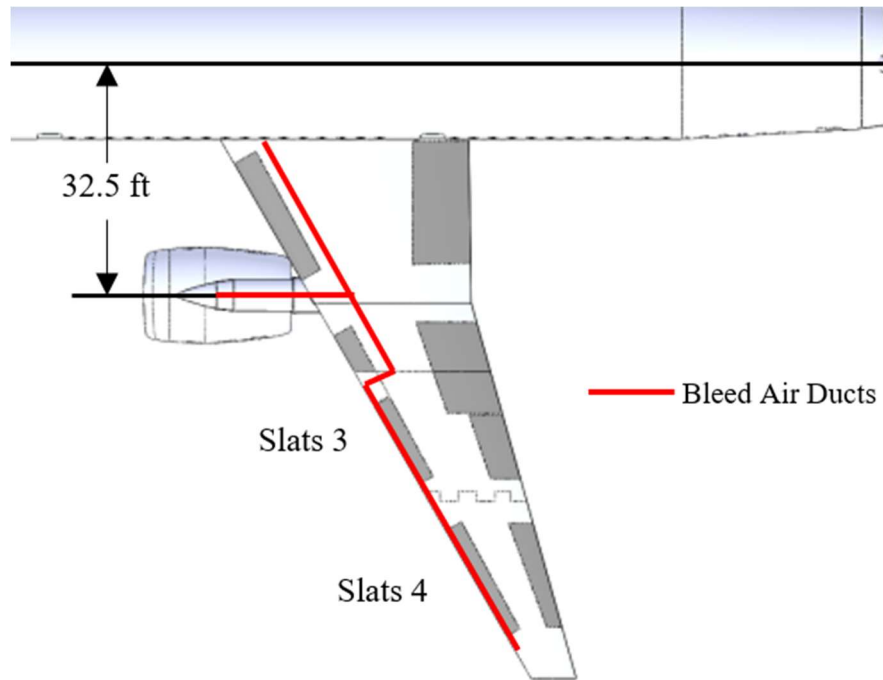


Figure 39 - Engine Installation and Anti Ice System

10.0 Aircraft Innovation: Folding Wingtip

As shown below in **Figure 40**, the Songbird can fit into group IV gates without any problems. As shown below in **Figure 40**, the Songbird can fit into group IV gates without any problems. This would allow it to compete with similar size aircrafts such as the B767-300. However, it will not be able fit into gates utilized by the B737 and the A320, which are the major competitors to this aircraft in the 700 nmi range mission. The Songbird's wingspan is about 54 ft longer than is allowable by category III gates and will intrude into adjacent spaces, as show below in **Figure 41**. The Songbird's wingspan is about 54 ft longer than is allowable by category III gates and will intrude into adjacent spaces, as show below in **Figure 41**. The folding wing tips, shown below in **Figure 42**, were chosen as a design innovation to reduce the wingspan during taxi and resting position. The folding wing tips, shown below in **Figure 42**, were chosen as a design innovation to reduce the wingspan during taxi and resting position. This innovation was incorporated into the design to fold the wingspan a total of 54 ft and allow it fit into category III gates.

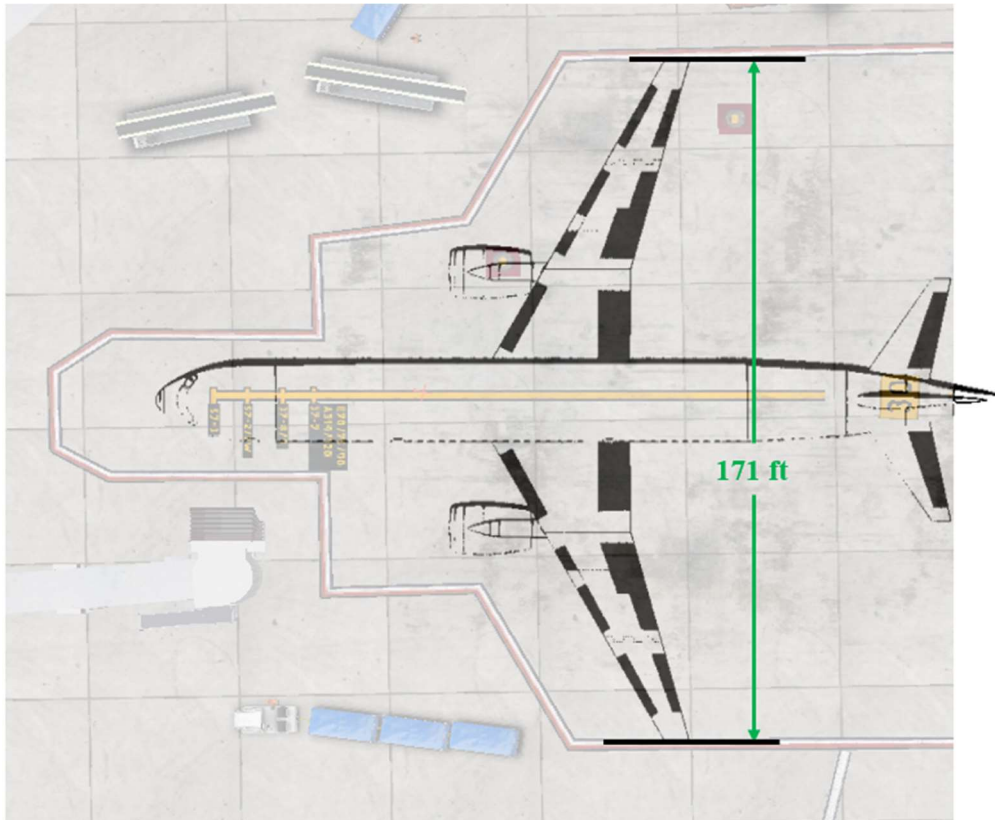


Figure 40 - Category IV Gates can Accommodate the Songbird

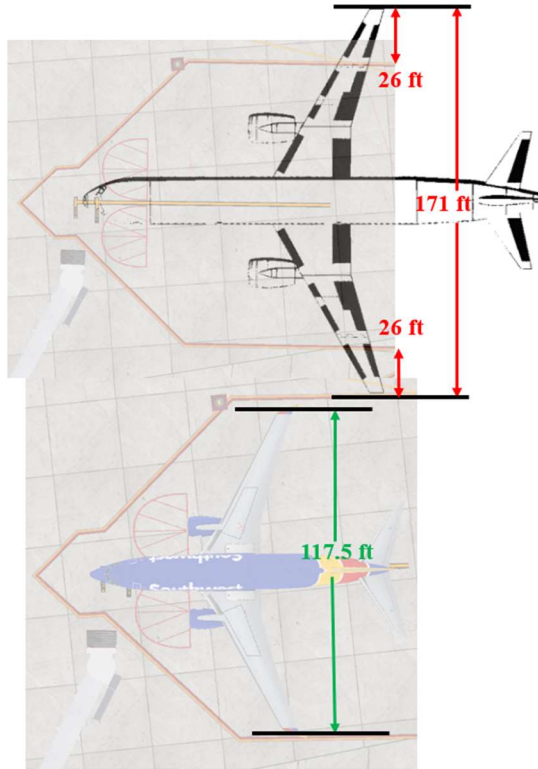


Figure 41 - Songbird Wingtips Encroach 27 ft into Adjacent Spaces

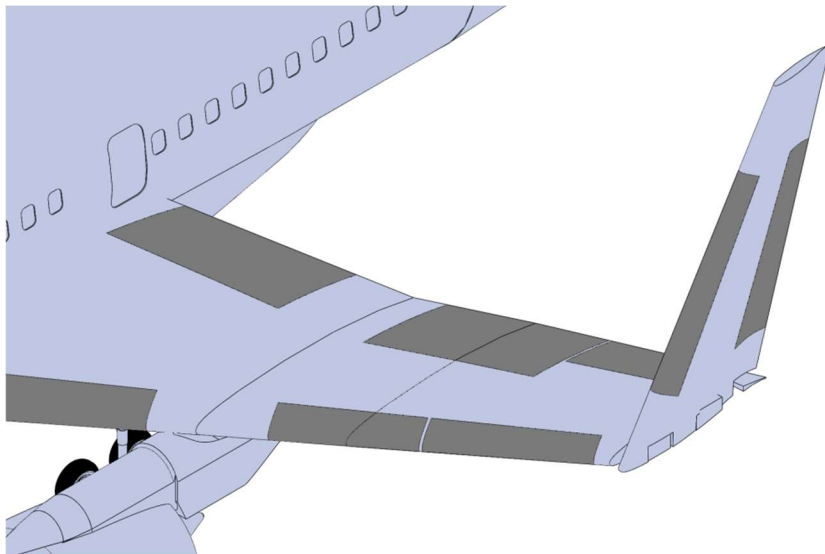


Figure 42 - Aircraft Wingtips fold 27 ft on each side

11.0 Aerodynamic Characteristics and Performance

11.1 Airfoil Selection

The airfoil selection was critical to the design of the main wing in which determined if the wing would produce enough lift for the Songbird, given the weight and speed requirements of the mission. Different supercritical airfoils were analyzed due to the thickness distribution and high camber in the aft section of the airfoil. The 3 supercritical airfoils analyzed were the NASA (2)-0518, NASA (2)-0712, and NASA (2)-1010. The airfoil chosen was the NASA (2)-0712. This was due to the airfoil having both traits desired from its competing airfoils that were analyzed. The NASA (2)-0518 had the right thickness, given the Songbird's requirements, however, lacked in the camber aspect as shown below in **Figure 43**. The NASA (2)-1010 shown in **Figure 44** had higher camber which was favorable for the Songbird's lift and functionality of control surfaces like flaps, allowing smaller flap lengths needed to be deployed. However, this airfoil had a thickness that was not able to fit the internal volume requirements for the fuel stored in the wing. This then led to the final selected airfoil, the NASA (2)-0712 seen below in **Figure 45**, which fit both the thickness and camber aspects desired for the main wing.

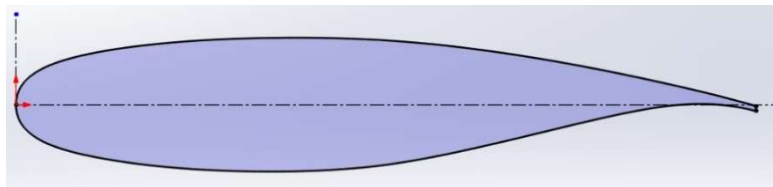


Figure 43 - NASA (2)-0518 Airfoil

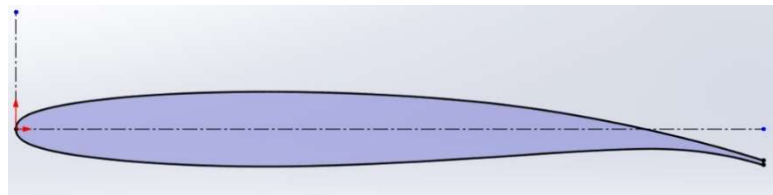


Figure 44 - NASA (2)-1010 Airfoil

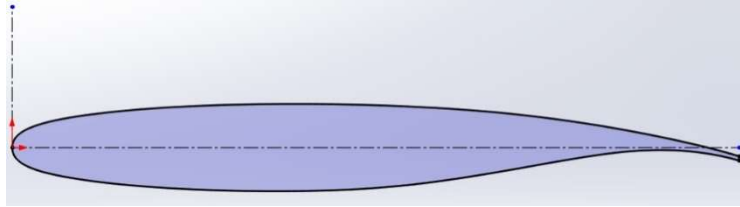


Figure 45 - NASA (2)-0712 Airfoil (Final Airfoil Selected)

11.2 Lift Curve Slopes

The low-speed lift curves are shown in **Figure 46**. These lift curve slopes account for all configurations with the use of flaps and slats. These lift curve slopes are significant in showing how the use of different configurations with control surfaces can change the lift during different conditions of flight. **Figure 46** shows that with the use of flaps and slats extended during takeoff, landing, or cruise, the C_{Lmax} increases, therefore, allowing the angle of attack for stall to be higher than the stall angle of attack without these configurations. One thing to note was that for all configurations, the C_{Lmax} occurred before the tip back angle limit. This is interpreted to prove that the Songbird can take off and land at an angle of attack lower than the tip-back angle, preventing a tail strike under these flight conditions.

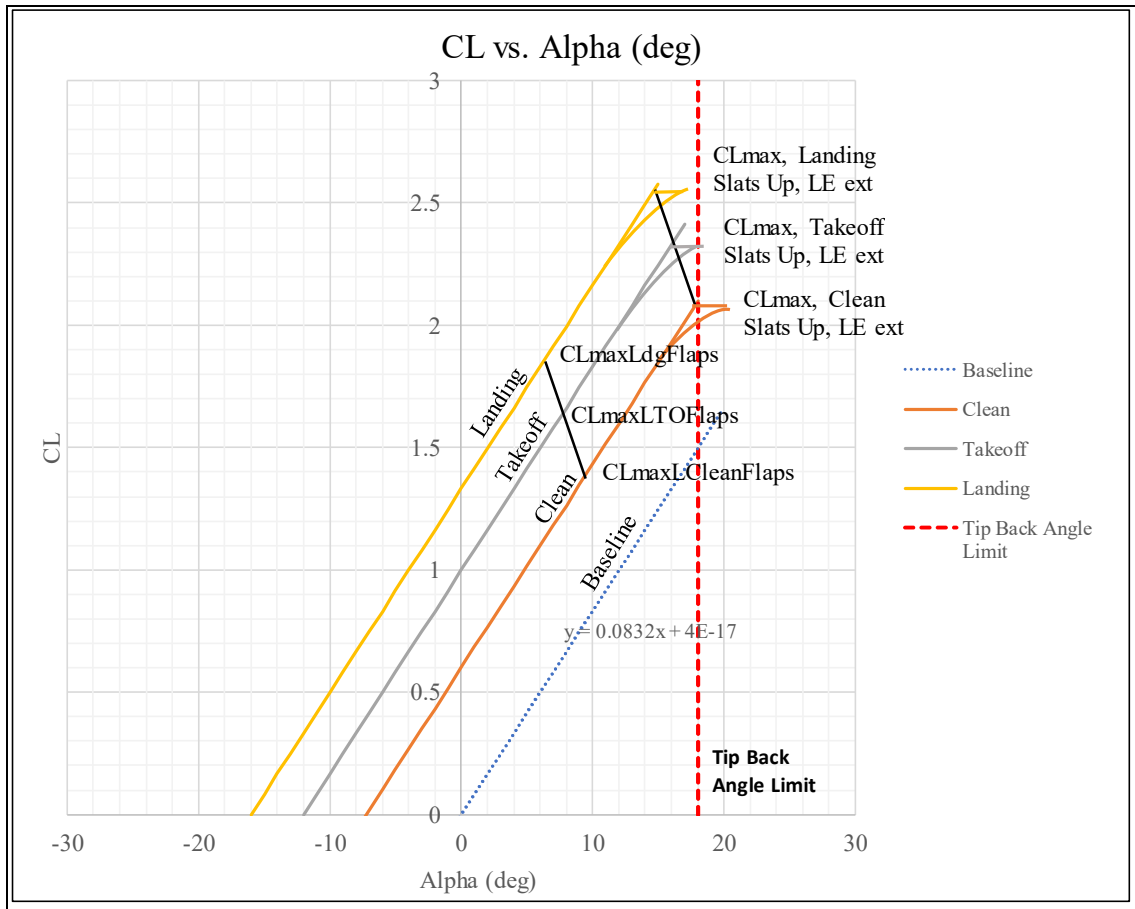


Figure 46 - Low-Speed Lift Curves for all Configuration

11.3 Drag Polar

The drag polar curves shown below in **Figure 47** and **Figure 48** were significant in showing the relations between drag and lift under different flight conditions and configurations. The drag polar is able to be interpreted for the aerodynamic efficiency of the aircraft as it is desirable to have the highest amount of lift with the lowest amount of drag possible. The black “x” marks represent the cruise condition L/D. The L/D_{max} for the Songbird was calculated to be 20 while the Songbird’s cruise condition L/D was 18 (86.6% of $L/D_{max} = 20$), due to it being powered by jet engines. [2] The Songbird based off this data is seen to be aerodynamically efficient considering the short- range mission the aircraft will operate for.

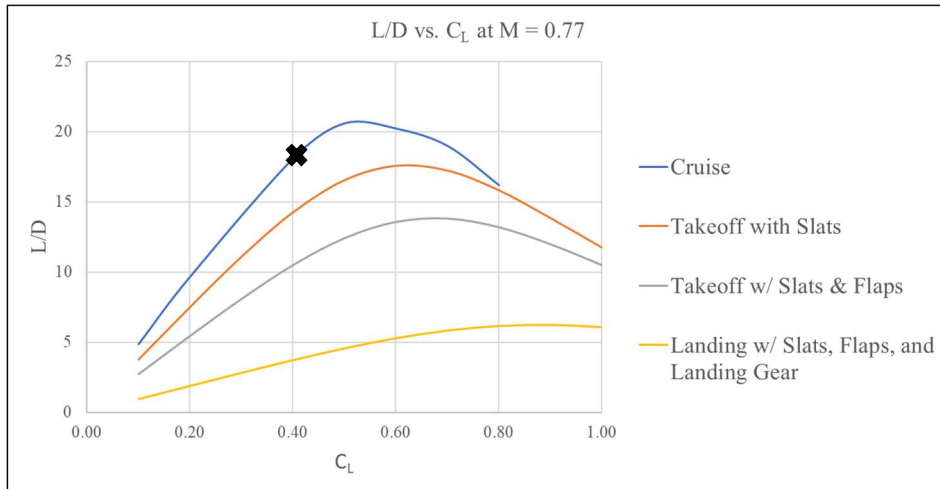


Figure 47 - Lift-to-Drag Ratio vs. Lift Coefficient at Mach = 0.77

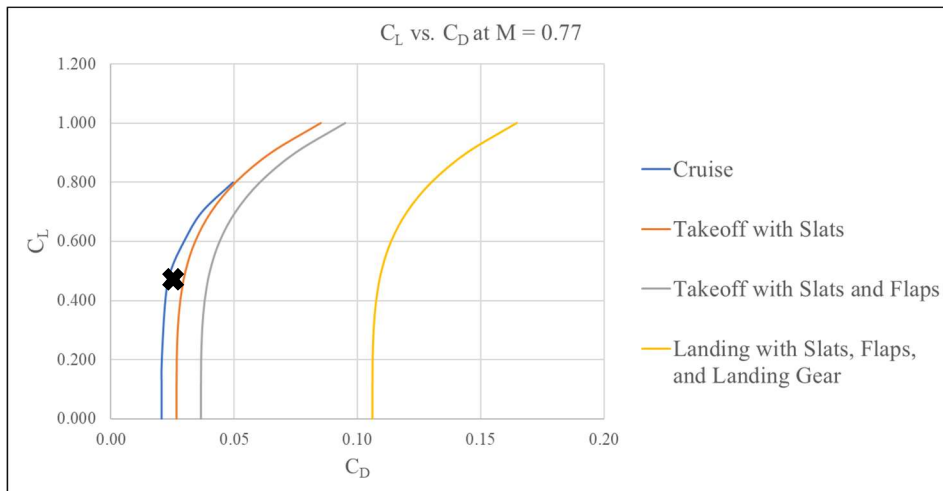


Figure 48 - Lift Coefficient vs. Drag Coefficient at Mach = 0.77

12.0 Performance

12.1 Takeoff Field Length

Takeoff analysis was conducted using the method described by Schaufele. To comply with the RFP, the analysis was calculated at sea level ISA + 15 °C with the following parameters shown in **Table 14** below. In case one engine fails during takeoff the takeoff must be a balanced field length, which is where the distance needed to stop from takeoff roll is equal to the distance needed to continue the takeoff. The balanced field length, calculated below in **Figure 49**, is 5900 ft and complies with the RFP requirement of landing under 9000 ft.

Table 14 - Takeoff Parameters

Parameters	Symbol	Value
Rolling Coeff	μ_R	0.03
Braking Coeff	μ_B	0.3
Wing Area	S	3246 ft ²
Total Thrust	T	130000 lb _f
Max Takeoff Weight	MTOW	386800 lb
Wing Loading	W/S	120
Thrust to Weight	T/W	0.30
Max Lift Coeff	$C_{L\ max}$	2.54
Density (ISA + 15)	ρ	0.00225955 slug/ft ³
Takeoff Speed	V_{TO}	145 kts
Stall Speed	V_s	120 kts

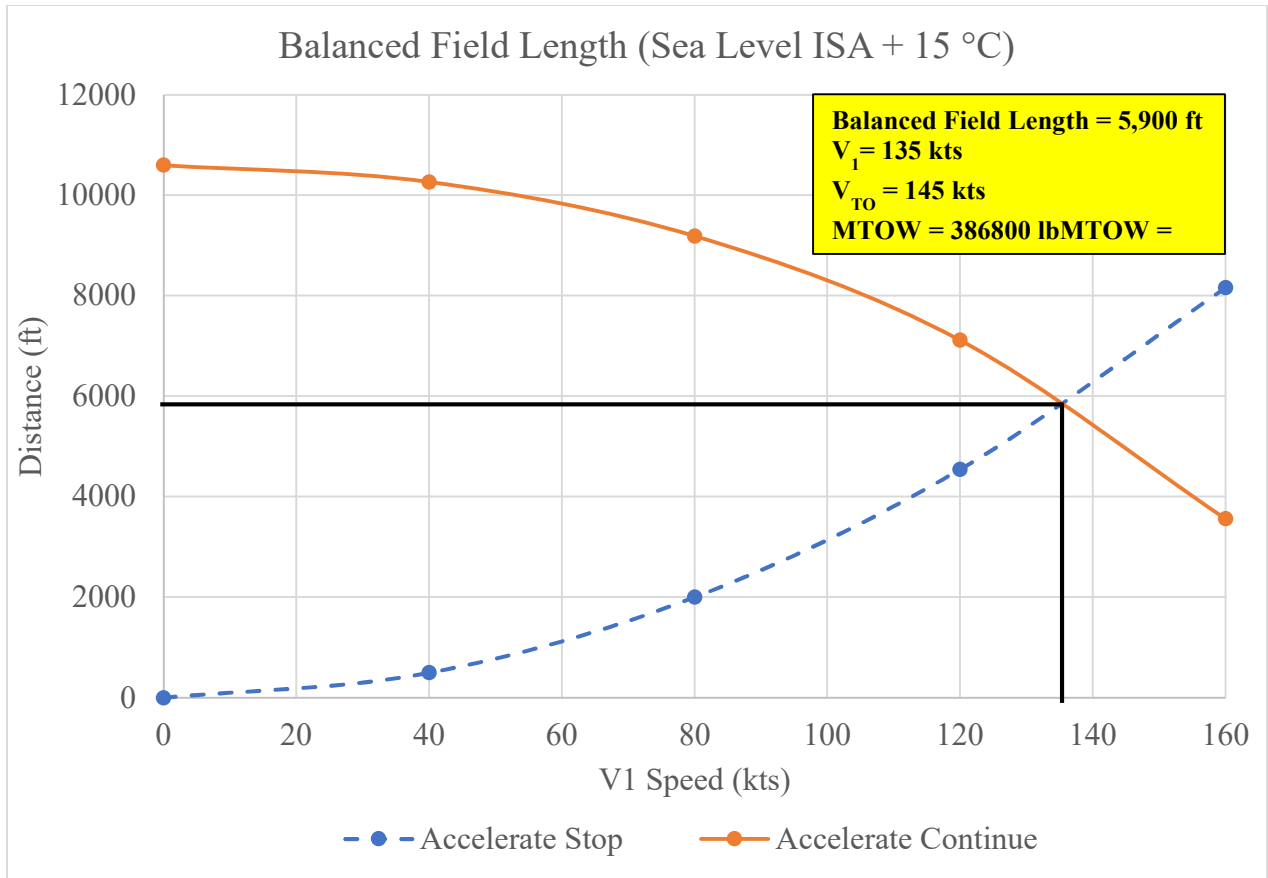


Figure 49 - Takeoff Length is a Balanced Field of 5900 ft

12.2 Landing Field Length

The landing field analysis was conducted using the method discussed by Nicholai and Carichner. The landing field length was calculated at sea level ISA + 15 °C, as per the RFP. The aircraft was assumed to have a glide slope of 3 degrees with half the fuel remaining from MTOW. This resulted in a landing distance of about 3012 ft as shown below in **Figure 50**. The aircraft complies with the requirement of landing in under 9000ft. However, the approach speed does not meet the tradable requirement of 145 KCAS. Approach speed of the aircraft is about 153 KCAS.

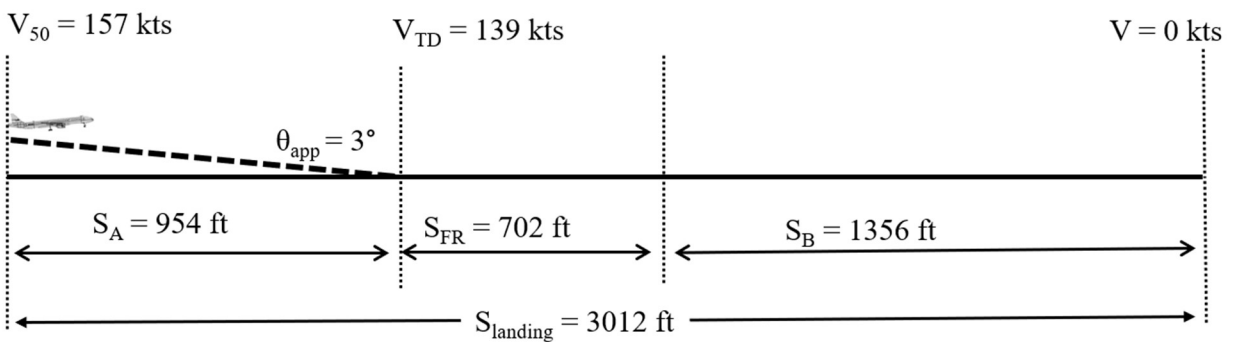


Figure 50 - Landing field at Sea Level ISA + 15 °C is 3012 ft

12.3 Flight Envelope

An operational envelope for the Songbird was calculated and shown below in **Figure 51**. The aircraft has a max ceiling of about 36,000 ft. The Songbird is optimized to cruise at an altitude 30,000 ft and a Mach number 0.77, which are all within the operating envelope.

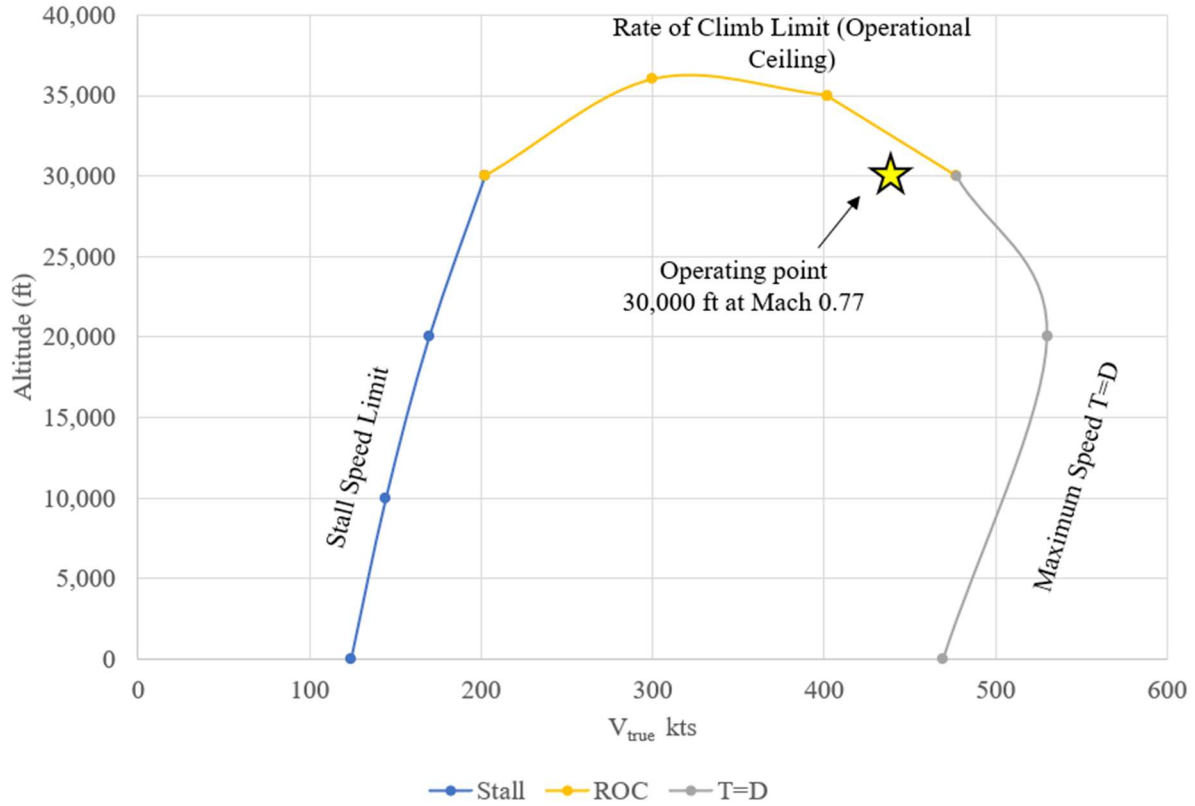


Figure 51 - Operational Envelope for Songbird

12.4 Payload Range

Shown below in **Figure 52** is the payload range chart for a 3,500 nmi mission plus a 200 nmi reserve fuel. This shows the relationship between the payload and the range for the Songbird. The range result for this mission meets the range requirement of the RFP. This could be due to the aircraft's unique design. The payload refers to all the mass that is taken by an airplane, excluding fuel. The structure of an aircraft is designed in order to be sustain a certain number of loads and the star on the plot shows the max range when this aircraft is configured with a full capacity of fuel and payload. Once arrived at such point, any further range is achieved only by reducing the payload, which follows a nearly linear relationship. Still, the amount of fuel that an airplane can carry is also limited. That is the reason that at one sudden point, the linear relationship changes drastically.

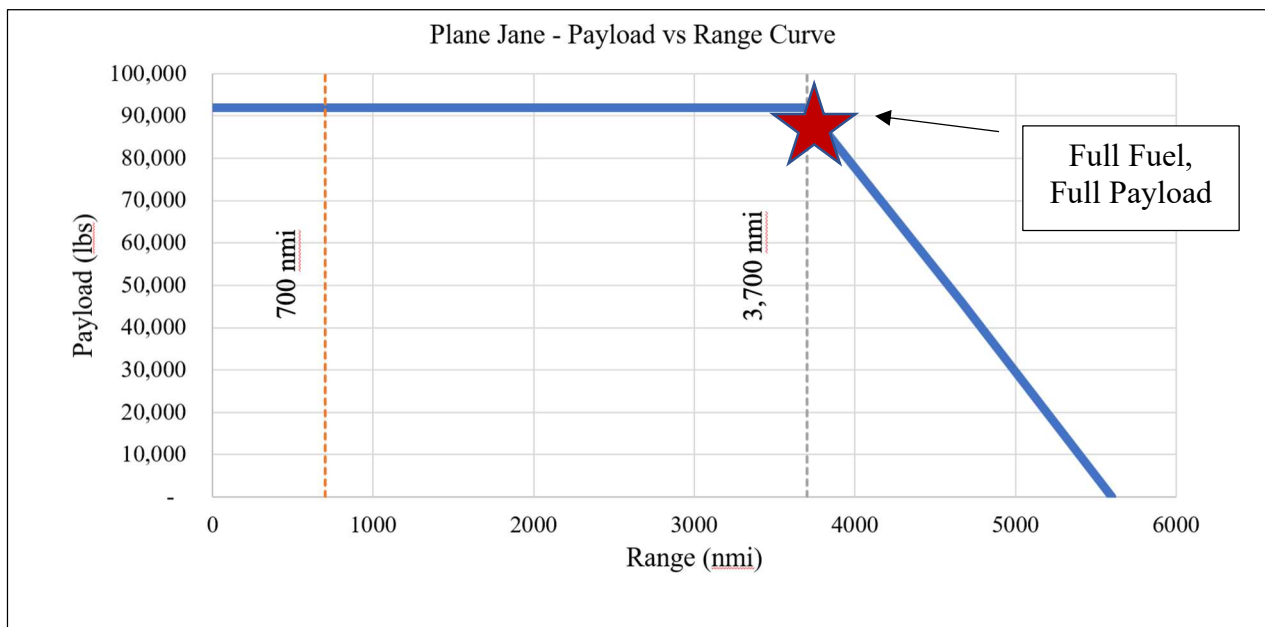


Figure 52 - Payload vs Range Curve

13.0 Structures

13.1 V-N Diagram

The structural analysis of the aircraft started with the construction of a V-n diagram in cruise condition, 30,000 ft altitude, at Mach 0.77 and with a MTOW of 389,550 lbs. The V-n diagram for the Songbird is shown in **Figure 53**.

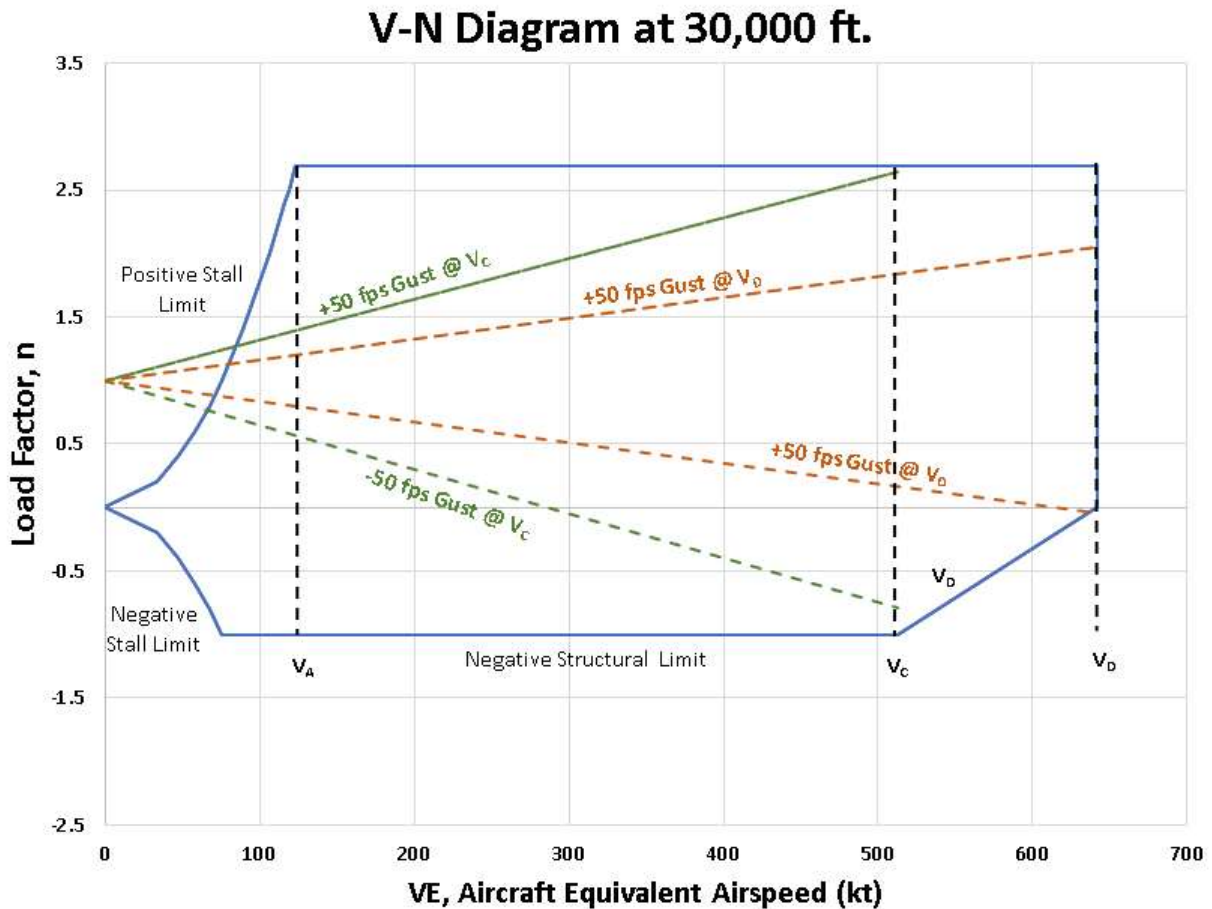


Figure 53 - V-n gust diagram at 30,000 ft

The aircraft is assumed to be in its clean configuration without flaps or slats deployed. FAR part 25 was used to calculate design speeds for stall, cruise, and dive speeds as well as maximum gust intensity. Cruise and dive speeds and 513.12 and 641.4 kts. respectively. The maneuver load factors were analytically calculated, with the positive load factor only varying with maximum takeoff weight. The negative max load factor for a transport aircraft like ours is mandated as -1 by FAR 25. Similarly, the gust loads were determined from FAR 25 and were reduced linearly to cruise altitude as shown in the green and orange lines. The V-N diagram shows that our

architecture will experience maximum maneuver loads of 2.7 and -1. The diagram also shows that the gust loads are not critical to the aircraft's structural integrity because they remain in the maneuver envelope.

13.2 Spar and Rib Sizing

Due to the large surface area of the wing and considerations from Roskam [19], a multi-spar wing box design is chosen, and the overall wing structure is relatively conventional and can be seen in **Figure 54**.

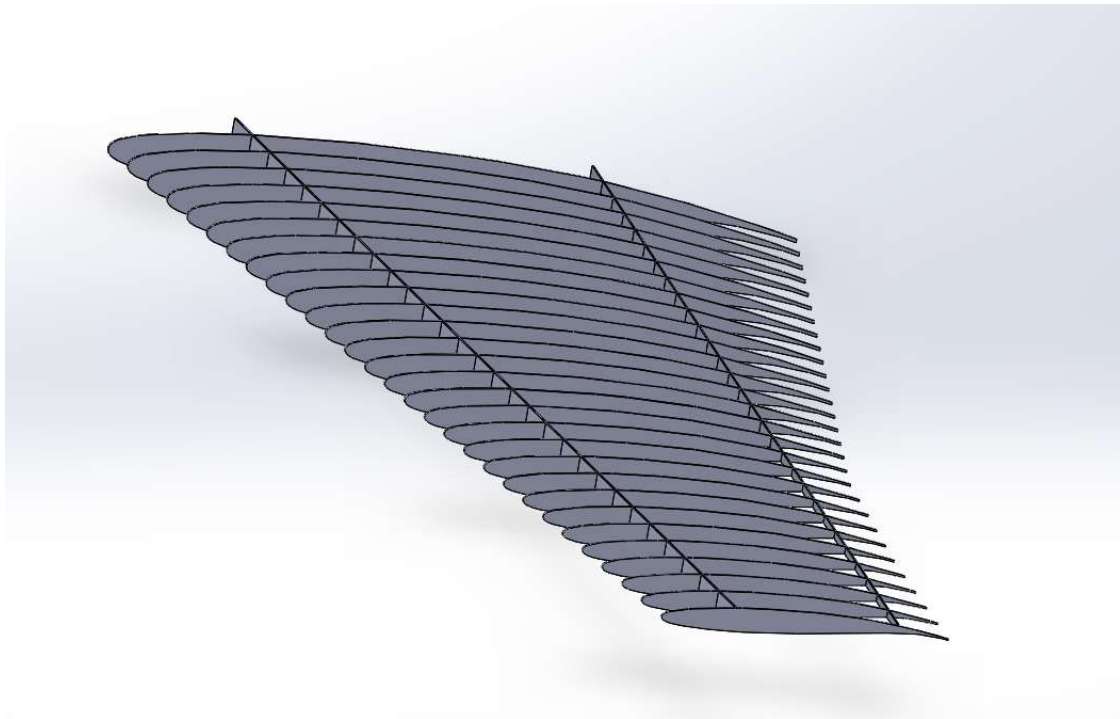


Figure 54 - Wing Box Structure Configuration

Roskam advises that for typical transport jets the front spar be at 15-30% of the chord and the rear spar to be at 65-75% of the chord. In order to accommodate for the fuel tanks and the required control surfaces, a two-spar design was chosen with the front and rear spar located at 15% chord and 70% chord respectively. Roskam recommends a 24-inch rib spacing for transports, however due to the folding wing tips and the availability of statistical data of modern transport jets a different spacing was chosen. Following data from a 2004 statistical study conducted by NASA Langley Research Center and Embry-Riddle Aeronautical University, the rib spacing was chosen

to be 20 inches [20]. The same statistical data will be followed for the wingbox; thus, the spar and rib thickness are 0.05 and 0.08 inches respectively.

13.3 Material Selection

The Songbird's material composition follows industry trends and modern structural philosophy. For this architecture we chose to make use of high strength composite materials for the high lift devices, doors, and fuselage skin which brought the usage to around 65%. Such a high percentage of composite usage was chosen due to their weight savings and the increasing rate at which composites are being adopted and validated in the aerospace industry. According to Nicolai and Carichner, a composite wing will on average save 20% weight when compared to conventional steel alloys. The composite chosen was carbon fiber reinforced polymers due to their widespread validation in existing aircraft.

However, mechanical and load bearing structures like the landing gear will still use conventional steel (aluminum, titanium, etc.). This is due to composite structures not being impact tolerant and their tendency to fail without warning. Therefore, the ribs and wing spars are made of titanium, while the skin of aircraft will be composed of carbon fiber reinforced polymers. However, locations where impact from debris is likely will not employ composites. The areas likely to experience debris damage are the front of the wings and tail; thus, aft of the 15% chord will be composed of aluminum. Behind the 15% chord, the wing skin will be made from carbon fiber reinforced polymers.

14.0 Landing Gear

The main landing gear is designed to absorb 85% of the MGTOW and will be installed behind the aircraft's CG. This architecture's landing gear was designed to avoid any rupture leading to the spillage of enough fuel to constitute a fire hazard as a result of a wheels-up landing on a paved runway set by Part 14 sec 25.721(b).

14.1 Landing Gear Placement

A non-fixed tricycle-type landing gear was selected due to its structural integrity and this configuration's ability to provide our architecture with a lower overall operating and manufacturing cost. In addition, this non-fixed configuration when deployed increases the overall drag on the aircraft along with increasing the possibility of gear malfunctions when deploying or retracting the landing gear. In **Figure 55** it can be seen for our design the non-fixed retractable, tricycle type landing gear was known to be a traditional configuration for this type of transport aircraft.

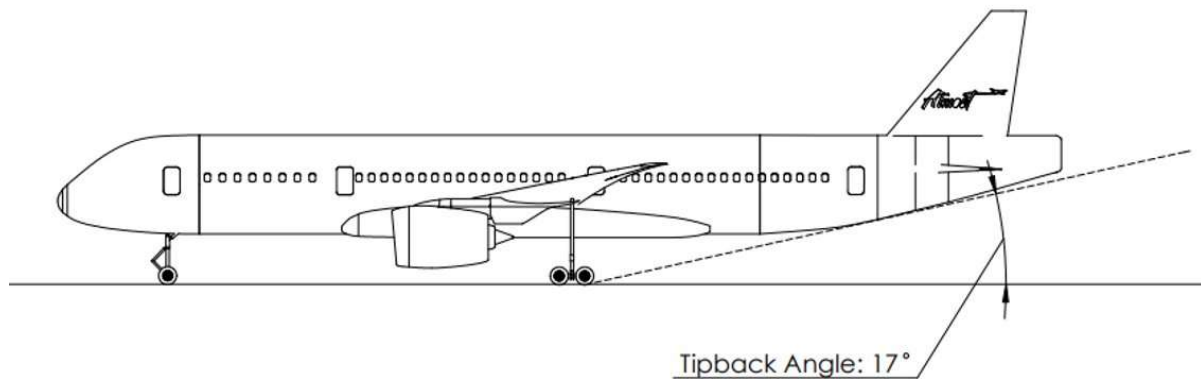


Figure 55 - Landing Gear Placement

14.2 FAA Requirements for Tip back/ Roll Over etc.

The rear landing gear is to be positioned to have a tip back angle of 17 degrees along with an C.G. to the rear landing gear of also 17 degrees. Also, shown in **Figure 56** for our architecture we have a turnover angle of 53 degrees which is less than the FAA requirement of 25-63 degrees. The tip-back angle is important to ensure that the aircraft's control surfaces along with the fuselage do not collide with each other or the pavement.

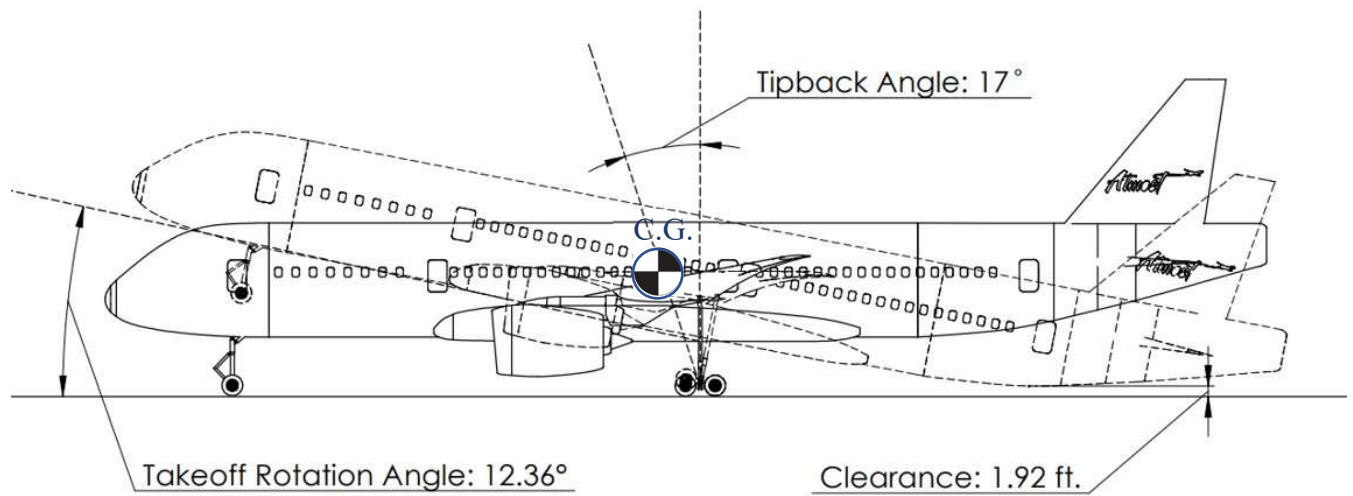


Figure 56 - Architectures' Takeoff Rotation Angle and Clearance

Figure 57 and **Figure 58** shows the maximum roll angle clearance of 16.6 degrees along with the angler clearance of 4.6 degrees, and an overturn angle of 63 degrees. As stated previously, these calculated values are in operating standards that satisfy the FAA requirements.

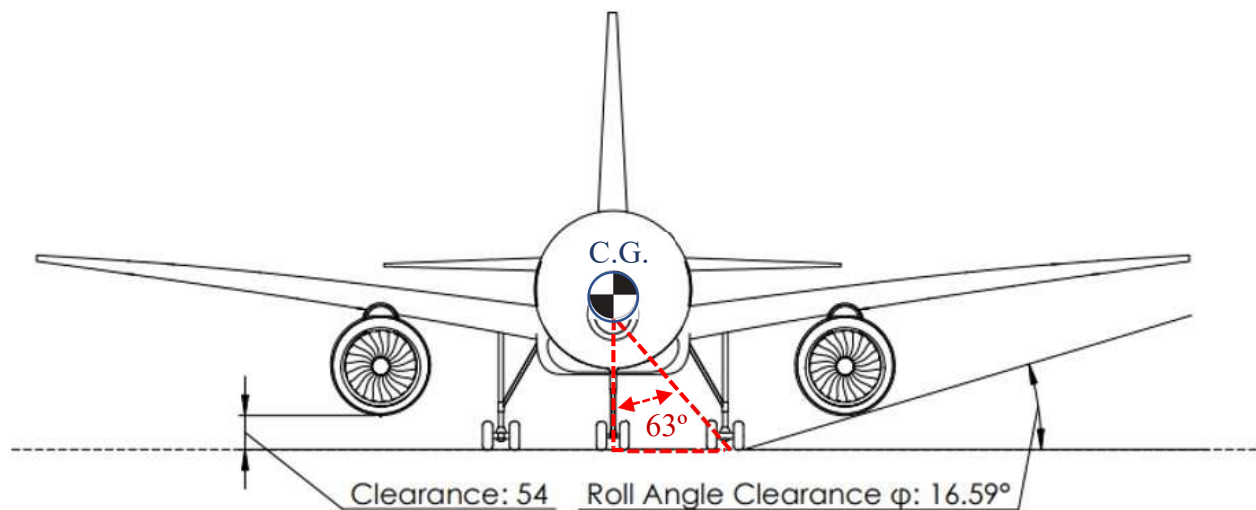


Figure 57 - Landing Gear Overturn Angle

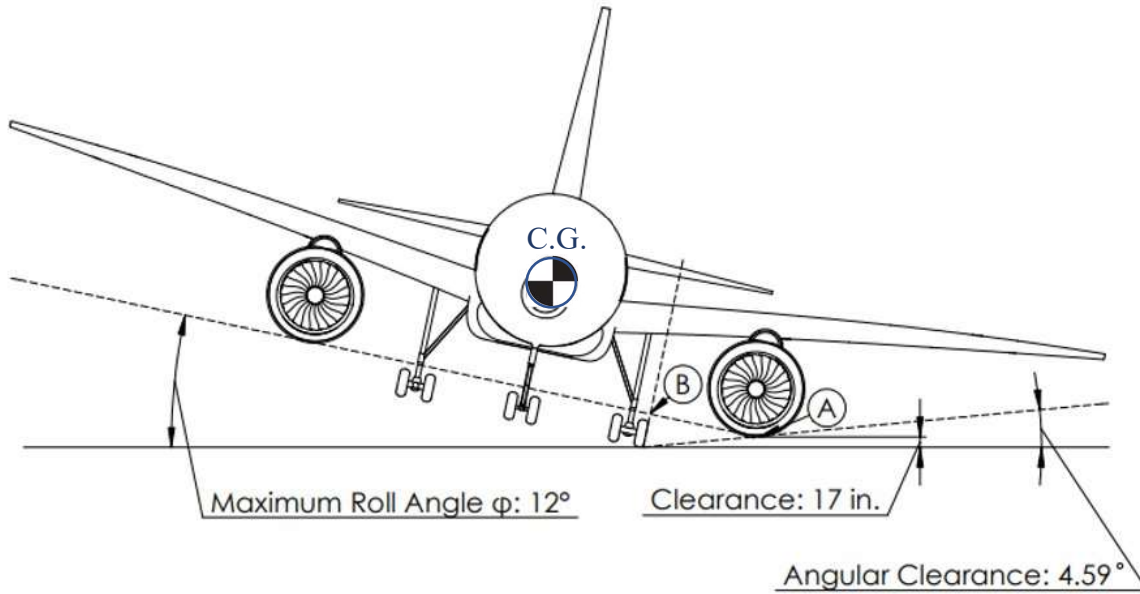


Figure 58 - Maximum Roll Angle with Angular Clearance

14.3 Tire selection

Table 15 - Tire Selection Table

Tire Size Selection	Nose	Main	TYPE VII Tires
Manufacturer	GoodYear	GoodYear	
Tire Size (in x in)	(39 x 11)	(49 x 17)	
Rated Inflation (psi)	115	210	
Catalog #	00537	00537	
Actual Load (lbf)	22811	49535	
Rated Load (lbf)	25800	50400	

15.0 Stability Control

The stability characteristics for the initial stability characteristics were generated using the design point chosen from the constraint diagram, with all analysis regarding controls being based on its accompanying wing loading and thrust-to-weight ratio.

15.1 Notch Chart

A notch chart was generated to select the initial horizontal tail volume. The chosen tail volume coefficient for the horizontal tail is 0.7, as shown in **Figure 59**. This value was chosen to allow for a high tolerance in CG travel to meet the requirements for takeoff and landing maneuvers. The black line represents the CG travel margin at around 10 % of the leading edge Mean Aerodynamic Chord, while the blue line above it represents the “actual” CG travel at 5%.

15.2 Control Surface Placement

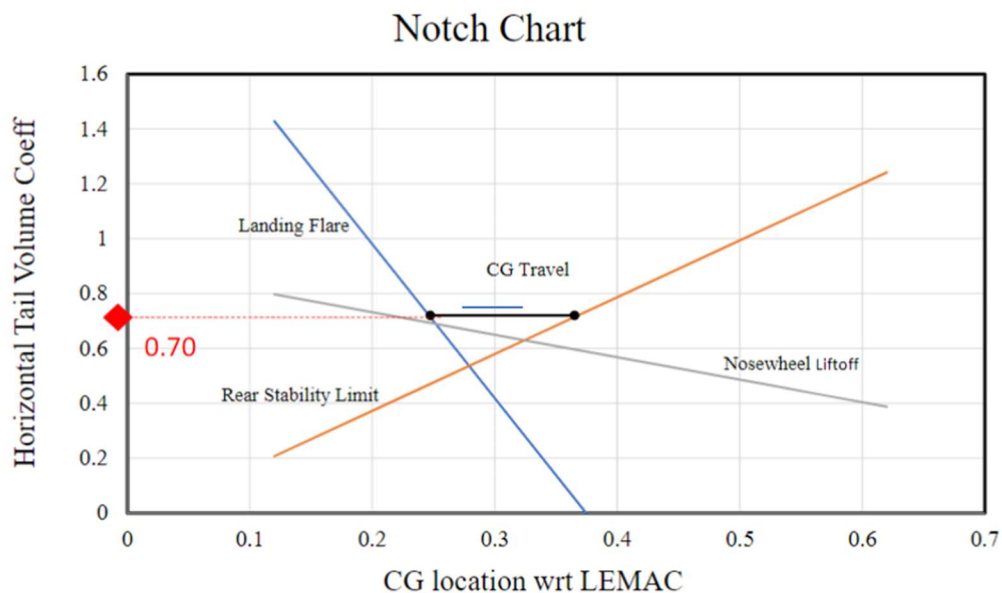


Figure 59 - Notch Chart Showing CG Travel

The placement of each of the control surfaces for the Songbird are shown below in the CAD model in **Figure 60**. The placement of the control surfaces was used in finding the stability conditions at various flight conditions.

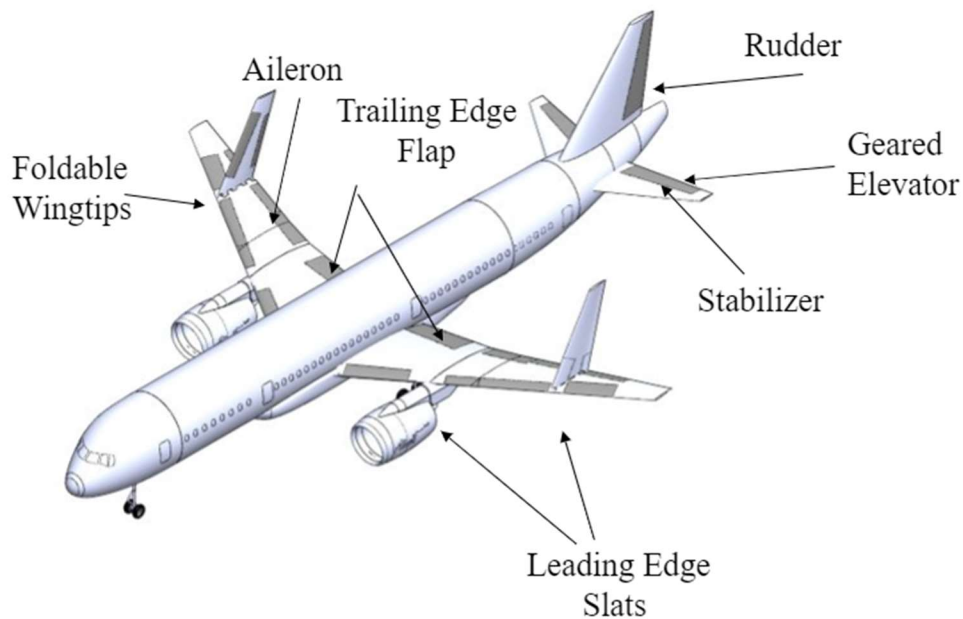


Figure 60 - Songbird Control Surface Placement

15.3 AVL Analysis

The horizontal tail volume coefficient was used as an updated input for the aerodynamic analysis tool called Athena Vortex Lattice (AVL) [7]. This tool was used to estimate the handling qualities of the aircraft regarding the dynamic flight modes and the corresponding stability derivatives of each aircraft. Stability characteristics were extrapolated from the excel and iterated through the modeling tool in AVL to render the architecture of the Songbird as shown below in **Figure 61**.

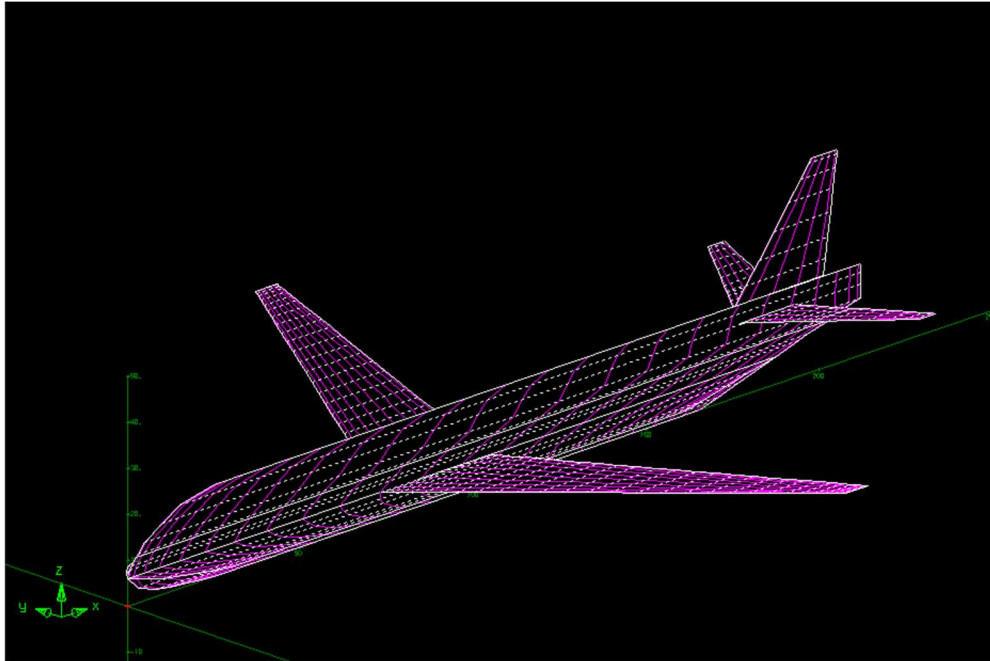


Figure 61 - AVL Model of Songbird

These models were used as the baseline for analysis regarding the stability and aerodynamics with both being continually updated through each design cycle up to the architecture selection phase. The sizing and placement of the tail and wing were also shifted to account for both aerodynamic performance and structural loading. All control surfaces shown in **Figure 61** were placed to match the CAD design file to ensure continuity in both the controls and structural aspects of the design.

15.4. Trim Condition

The Trefftz Plane Plot was useful in observing the estimate of the lift per span of the wing, as well as observing its elevator deflection in various flight conditions. The trim condition is shown in the Trefftz Plane Plot below in **Figure 62**. The trim condition shown is assuming cruise conditions at a Mach of 0.77 and an altitude of 30,000 ft. The neutral point was found to be 107 feet from the nose of the aircraft. The static margin for the Songbird was found to be 13 % of the Mean Aerodynamic Chord, showing that the aircraft has suitable longitudinal stability at an analytical level.

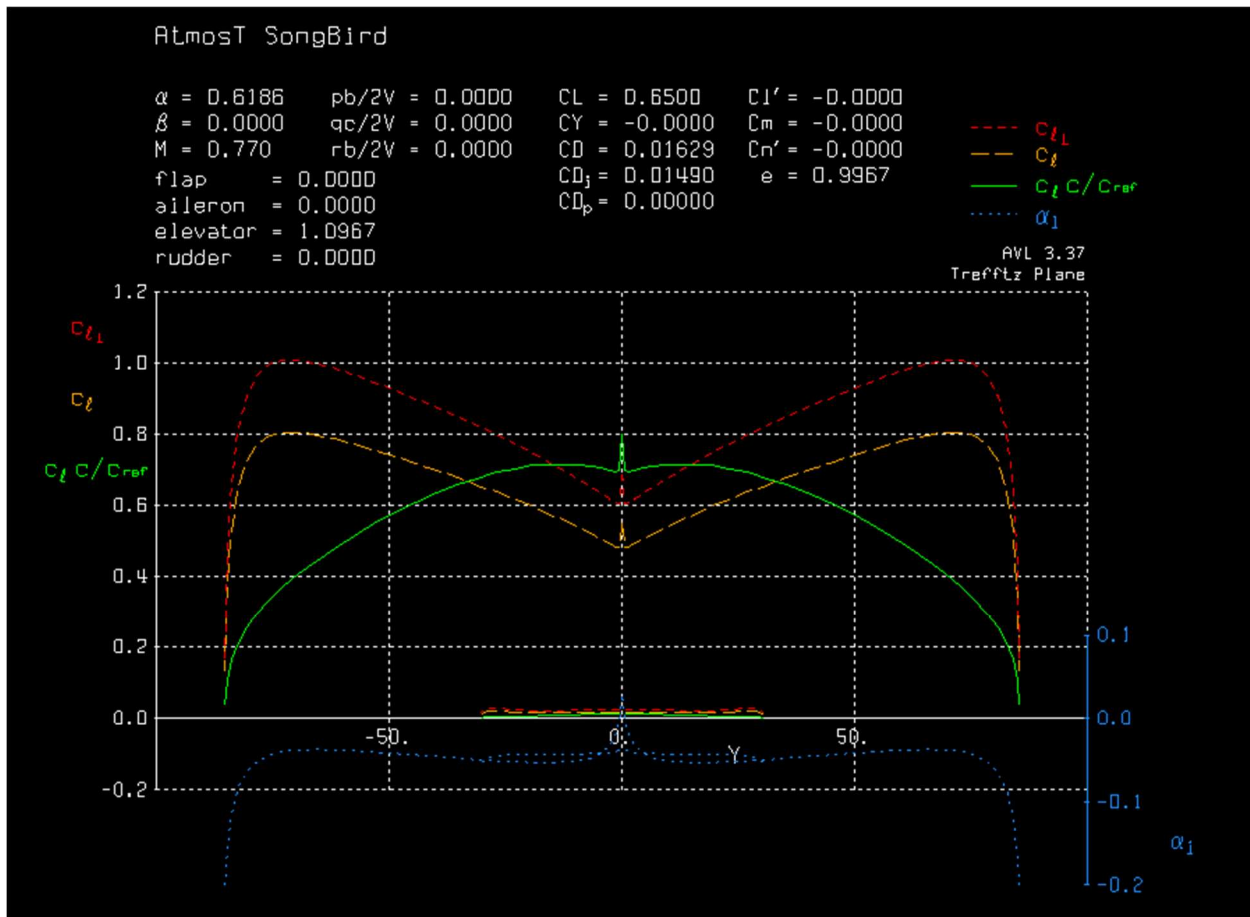


Figure 62 - Trefftz Plane Plot of Songbird

The observed trim condition for the aircraft has an angle of attack of about 0.6° with an elevator deflection of about 1.1° . It is important to note that AVL is optimized to calculate slender bodies and the addition of the fuselage was yielding unexpected results. Because of this, the fuselage was removed when analyzing the trim condition. The low amount of elevator deflection signifies a low amount of user input required for stable flight, which is optimum in terms of handling qualities. AVL was integral in giving a preliminary check on the location and volume coefficients of the stabilizers and helped to influence important decisions through each iteration. One of these important decisions was to increase the incidence angle of the wing section to increase longitudinal stability. The positioning of the wing, CG, and tail sections were changed due to the output of AVL, which caused a dramatic increase in stability at the operated flight envelope.

15.5 Stability Derivatives

The stability derivatives for the Songbird assume the cruise condition of $M = 0.77$ and 30,000 feet. The values were generated using AVL and were used as a check of the lateral and longitudinal stability derivatives. The stability derivatives are shown below in **Table 16**. These values were compared to those of an existing aircraft as a preliminary check, with its comparison to the Boeing 747 shown below in **Table 17** [14].

Table 16 - Stability Derivatives of Songbird

Table 14.5-1 Stability Derivatives of Songbird

HCSR Songbird: @ 30,000 ft., $M = 0.77$			
Longitudinal	$C_{L\alpha}$	$C_{m\alpha}$	C_{mq}
	5.120	-2.231	-30.11
Lateral	$C_{y\beta}$	$C_{n\beta}$	C_{nr}
	-0.926	0.1469	-0.6287

Table 17 - Stability Derivatives of Boeing 747

Boeing 747: @ 40,000 ft., $M = 0.90$			
Longitudinal	$C_{L\alpha}$	$C_{m\alpha}$	C_{mq}
	5.70	-1.26	-20.8
Lateral	$C_{y\beta}$	$C_{n\beta}$	C_{nr}
	-0.85	0.20	-0.325

16.0 Manufacturability and Reliability

16.1 Manufacturability

AtmosT would like to establish main assembly plant near the East Coast to be able to serve airlines out in Europe and still be capable to fill the need for our Songbird aircraft in the United States. While the team has not finalized the selection of chosen location, it has been agreed that it be located at a state based on the offered incentives and tax breaks that will benefit AtmosT. According to a study done in 2019, Ohio is one of the top 10 states for number of announced economic incentives package, making it a strong candidate to establish our assembly plant.

The team would also be cautious about outsourcing aircraft components and will strive to manufacture majority of the aircraft components in-house, and only outsourcing whenever it is substantially beneficial to the team and the company and all within the United States. Historical data and events will be carefully reviewed to avoid any delays that other aerospace companies may have faced due to being heavily relying on outsourced labor, like the delays that the Dreamliner 787 program had greatly suffered from.

Figure 64 shows a preliminary manufacturing concepts that the team would be following with the goal of increasing production rate. AtmosT would also adapt to six sigma process to efficiently minimizing manufacturing and assembly time and that all workers and employees are at least six sigma green belt certified. Additionally, Engineers would always be available to on the assembly floor to tackle any issue that may present itself without leading to any delays. Efficiency will be further increased by consolidating individual aircraft parts to reduce both shipping cost and assembly time.

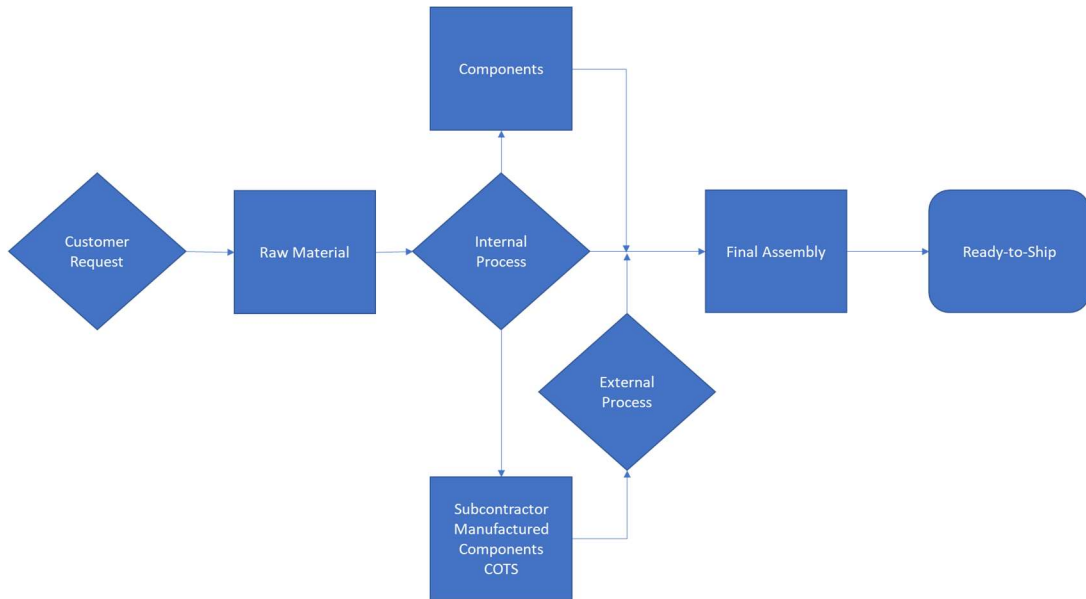


Figure 63 - AtmosT's Preliminary Manufacturing Concepts

16.2 Reliability

System reliability was used into all aspects of the design to ensure the maximum uptime of both production and mission time, with the lowest amount of failures possible. One of the ways this was incorporated into the design was through the conception of a flight control system up to FAR Part 25 requirements. The block diagram of the flight control system is shown below in **Figure 64**.

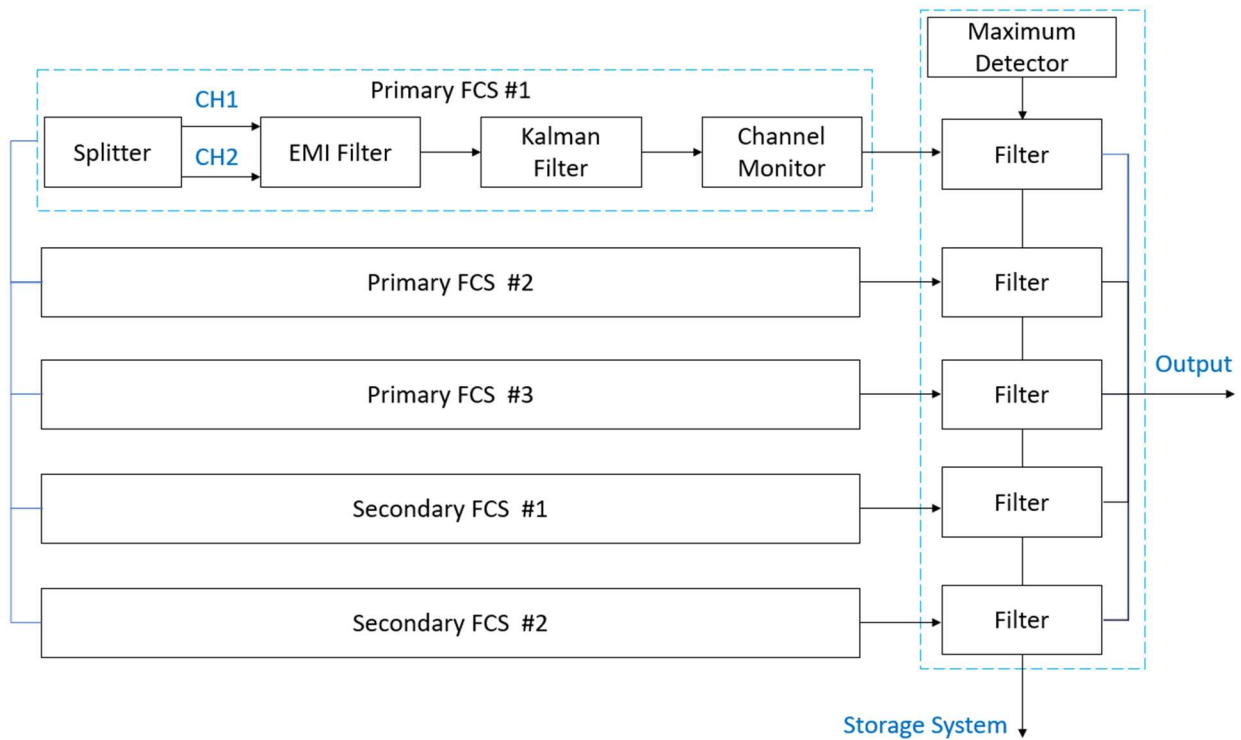


Figure 64 - Block Diagram of Flight Control System

The flight control system is quintuple-redundant and makes use of a detector to check if the active flight controllers are outputting any deviation outside of natural limits. This ensures that the flight controller is always operating correctly and lowers the risk of a critical failure if there is inconsistency in either the filtering or the output stage of the block diagram.

Ideally, each individual unit would be broken down into components with a corresponding Mean Time Between Failure (MTBF) to calculate the overall subsystem and system reliability for the aircraft. Although, Consumer Off the Shelf Parts (COTS) could be used to gather an MTBF at the product level, it would yield improper results because it fails to take real flight-hours into account. The Weibull distribution method has been chosen to simulate system reliability since MTBF requires flight data and failure occurrences. Below, the reliability of each subsystem has its corresponding system reliability shown below in **Table 18**.

Table 18 - Reliability Subsystem Breakdown

HCSR Songbird				
Subsystem	Alpha (hours)	Beta	Time (hours)	Reliability
Airframe	5.08E+04	2.90	13	0.99926
Electrical	5.61E+04	1.90	13	0.99956
Flight Control	4.38E+04	1.47	13	0.99956
Ground Control	2.68E+04	1.50	13	0.99927
Powerplant	4.97E+04	1.63	13	0.9996
System Reliability				0.9977

The chosen values for each subsystem are in accordance to a form factor of 2, with different factors like the Technology Readiness Level being used to estimate a scale for the chosen values. A time of 12 hours was chosen to account for the worst-case condition to simulate a maximum amount of flight hours for the alternate reference mission of 3500 miles with extra fuel for a divert. This same analysis was also done for the second candidate architecture. **Figure 65** shows a comparison of the Songbird to data of the Boeing 737 [18] and the second architecture.

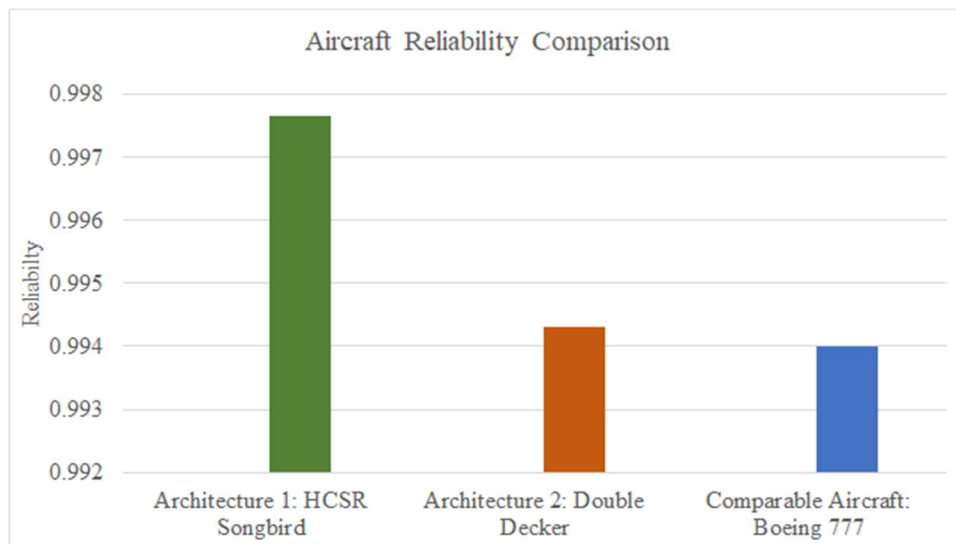


Figure 65 - Reliability Comparison to Existing Aircraft

17.0 Life Cycle Carbon Dioxide Emissions Estimate

Since the RFP calls for the design to take into an account a life cycle for carbon dioxide (CO₂) emissions estimate some requirements should be met to ensure our aircraft is designed to reduce the least amount of carbon emissions. This estimate includes (CO₂) emissions from manufacturing the aircraft, fuel burn rate of the aircraft as well as (CO₂) emissions from competing aircraft currently in service.

17.1 Research on finding equations and existing numbers

Calculating the carbon dioxide emissions of flights from five different airports selected from the mission marking study, it became increasingly important to establish where this aircraft ranked vs its competitors. Our design was geared towards reducing and monitoring the environmental impact the design had on the atmosphere. AtmosT used the traditional method for calculation of the amount of emissions that is emitted during transport travel. After calculating the amount of fuel burned, we were able to average cost per passenger seat mile and distance of crucial high demand routes to record total (CO₂) emissions into the atmosphere. It was discovered that the (CO₂) emissions was directly related to the fuel burn.

17.2 Emissions comparison with significance

From **Figure 66** it is found that our selected architecture ranked third compared to the competitors. This architectures' total emissions are about one ton less than that of the Douglas MD-88, which has a fuel burn rate of about twice as higher than our design. Nevertheless, our architecture is as an economically feasible aircraft and tremendous development and research went into manufacturing both a financial and economic aircraft to achieve optimum alternatives to existing aircraft.

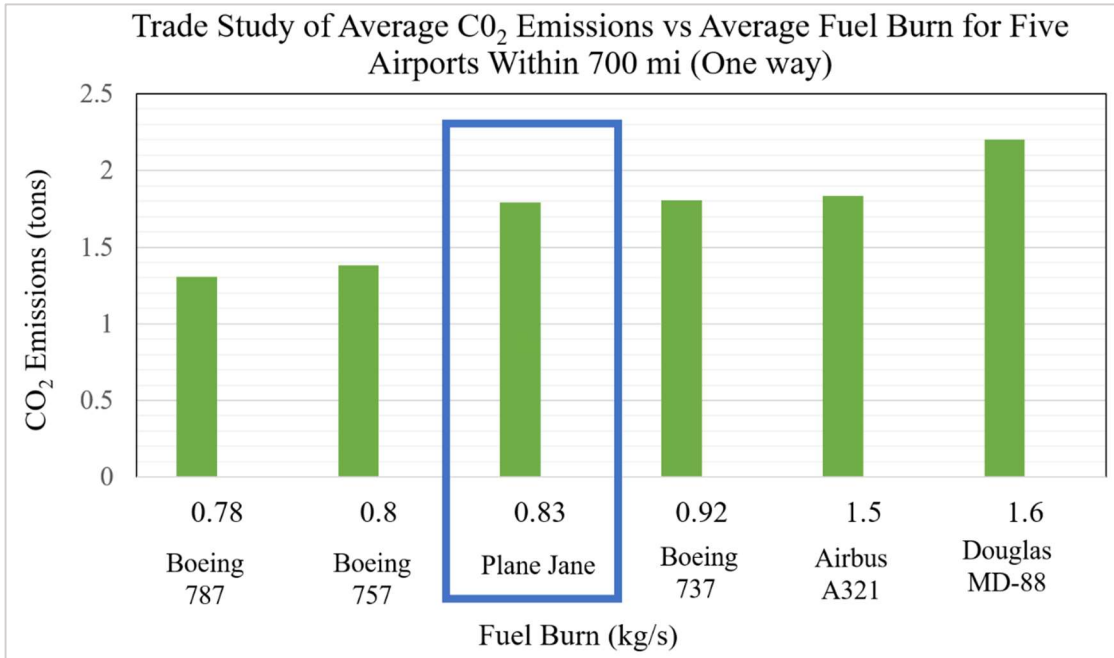


Figure 66 - CO₂ Emissions vs Average Fuel Burn

18.0 Conclusion

Songbird is better than the planes in development and in production to reduce congestion, increase safety at airports, reduce costs and EIS of 2029. Congestion can cause operational hazards such as ground collisions at key intersections at the airport taxiway/runway. This design was engineered to reduce congestion by studying gate utilization and ground ops activities to reduce to return time and increase overall safety. Gate utilization was an important design driver because we can offer less aircraft on the runway with the same passenger capacity as the competitors. This lead AtmosT to figuring out the most utilized gate at busiest airports and as a result the use of category three (CAT III) gate with the option to fix into a category four (CAT IV) gate due to future expansion will be optimal. The overall challenge here was to prove that it is possible through more analysis of the wing structure and materials to fold the aircraft wing and fit in (CAT III). The chosen design is birthed from the B777x which is a plane that is not constrained physically by its AR because of folding wing tips like the Songbird aircraft.

Songbird was designed to reduce congestion and all-around turn time starting from when the aircraft wheels go down to when the wheels go back up. By referring to section 3.2, which relates to the nominal duration of time spent at the airport from landing to takeoff, turn time was reduced. Following the critical path of deplaning, cabin cleaning and enplaning using model-based systems architecture which allows for high traceability between operational, functional, and physical architectures. Also, this is a highly customizable model that can be adapted to quickly get results.

AtmosT was able to reduce turn time by reducing the critical path and our design offers spacious seating configuration, side slip seating. The pros of side slip seating are that our design offers an increase in aisle width coupled with a dramatic increase in the productivity of cleaning staff, enplaning, and deplaning. The logic behind our design is that the more time the airplane is on ground, the less money you are making, this is congestion at the airport being reduced due to less aircraft being maintained at any given time. In addition, looking at the ground operation the critical path of deplaning cabin cleaning crew and boarding and deboarding seen to be the most time consuming. AtmosT found the best critical path and as a result using high slip seat will allow provide no cost to the design of the aircraft. This directly positively affects both scheduling along with manufacturability based of the entry into service date of 2029 the TRL level is very realistic. Another important design driver for our selection is direct operating cost. Our design has a lower

overall operating cost than our competing commercial airliners. Songbird has more cargo space than necessary, which means that even if the main cabin is not filled all the way, there is still room for profit.

References

- [1] Bruhn, E. F. Analysis and Design of Flight Vehicle Structures. Tri-State Offset, 1973.
- [2] Carichner, Grant E., and Leland M. Nicolai. Fundamentals of Aircraft and Airship Design. American Institute of Aeronautics and Astronautics, 2013.
- [3] “Code of Federal Regulations Part 25.” ECFR, www.ecfr.gov/cgi-bin/textidx?SID=ef1a9cb4ac051a045772746522a1e081&mc=true&tpl=/ecfrbrowse/Title14/14cfr23_main_02.tpl.
- [4] Boeing. “High Capacity Short Range Transport Aircraft.” *AIAA.org*, 2019, www.aiaa.org/docs/default-source/uploadedfiles/education-and-careers/university-students/design-competitions/33996-undergraduate-aircraft---high-capacity-short-range-transport-aircraft.pdf?sfvrsn=1bf74215_0.
- [5] Raymer, Daniel P. Aircraft Design: a Conceptual Approach. American Institute of Aeronautics and Astronautics, 2019.
- [6] “SolidWorks 2020 Education Edition.”
- [7] Drela, Mark. “AVL User Guide.” *MIT*, 12 Feb. 2017, web.mit.edu/drela/Public/web/avl/avl_doc.txt.
- [8] Lee, Minwo, and Li, Larry. “Analysis of direct operating cost of wide-body passenger aircraft: A parametric study based on Hong Kong”. CSAA, 27 May 2019. <https://www.sciencedirect.com/science/article/pii/S1000936119301244>
- [9] i3dthemes.com, Code7700. “Fuel Density Engineering.” *Fuel Density*, 28 Oct. 2005, code7700.com/fuel_density.htm#references.
- [10] “Rolls-Royce Trent 7000.” *Wikipedia*, Wikimedia Foundation, 28 Feb. 2020, en.wikipedia.org/wiki/Rolls-Royce_Trent_7000.
- [11] Bishop, Kristina C, and John R. Hansman. *ASSESSMENT OF THE ABILITY OF EXISTING AIRPORT GATE INFRASTRUCTURE TO ACCOMMODATE TRANSPORT CATEGORY AIRCRAFT WITH INCREASED WINGSPAN FOR IMPROVED FUEL EFFICIENCY*. May 2012, dspace.mit.edu/bitstream/handle/1721.1/71120/MIT_Wingspan_Thesis_Bishop.pdf?sequence=1.

- [12] ELDORADO. “Analysis: How Long Does It Take to Exit an Airplane?” *ELDORADO*, 14 Mar. 2018, www.eldo.co/how-long-does-it-take-to-exit-an-airplane.html.
- [13] Yeager, Melissa. “What Does It Take to Get a Plane Ready between Flights? American Airlines Shows Us.” *Azcentral*, The Republic | Azcentral.com, 15 May 2019, www.azcentral.com/story/travel/airlines/2019/05/14/how-long-it-takes-to-get-a-plane-ready-between-flights-airplane-turnaround-time/1123694001/.
- [14] *Flight Stability and Automatic Control*, by Robert C. Nelson, WCB, 1998.
- [15] Karhu O, Kansu P, Kurinka I. Correcting working posture in industry: a practical method for analysis. *Applied Ergonomics* 1977;8:199–201.
- [16] Marelli, Scott, et al. “The Role of Computer Simulation in Reducing Airplane Turn Time.” *Airplane Turn Time*, www.boeing.com/commercial/aeromagazine/aero_01/textonly/t01txt.html. [17] “Vitech Corp CORE 9” software
- [18] Tinseth, Randy. “737 MAX: A YEAR OF SERVING THE GLOBE.” *Boeing: Randy's Blog*, 22 May 2018, randy.newairplane.com/2018/05/22/737-max-a-year-of-serving-the-globe/.
- [19] Roskam, Jan. *Airplane Design Part III: Layout Design of Cockpit, Fuselage, Wing and Empennage*. Ottawa, Kan.: Roskam Aviation and Engineering, 1985. Print
- [20] Sensmeier, Mark & Samareh, Jamshid. (2004). A Study of Vehicle Structural Layouts in Post-WWII Aircraft. 10.2514/6.2004-1624.
- [21] “Expedia Travel: Search Hotels, Cheap Flights, Car Rentals & Vacations.” *Expedia.com*, www.expedia.com/.
- [22] Brandt, Steven A., et al. *Introduction to Aeronautics: a Design Perspective*. American Institute of Aeronautics and Astronautics., 2015.